Austrian Journal of Technical and Natural Sciences

№ 11–12 2019
November–December

PREMIER
Publishing

Vienna
2019

Austrian Journal of Technical and Natural Sciences

Scientific journal

№ 11–12 2019 (November–December)

ISSN 2310-5607

Proofreading Kristin Theissen

Cover design Andreas Vogel

Additional design Stephan Friedman

Editorial office Premier Publishing s.r.o.
Praha 8 – Karlín, Lyčkovo nám. 508/7, PSČ 18600

E-mail: pub@ppublishing.org

Homepage: ppublishing.org

Austrian Journal of Technical and Natural Sciences is an international, German/English/Russian language, peer-reviewed journal. It is published bi-monthly with circulation of 1000 copies.

The decisive criterion for accepting a manuscript for publication is scientific quality. All research articles published in this journal have undergone a rigorous peer review. Based on initial screening by the editors, each paper is anonymized and reviewed by at least two anonymous referees. Recommending the articles for publishing, the reviewers confirm that in their opinion the submitted article contains important or new scientific results.

Premier Publishing s.r.o. is not responsible for the stylistic content of the article. The responsibility for the stylistic content lies on an author of an article.

Instructions for authors

Full instructions for manuscript preparation and submission can be found through the Premier Publishing s.r.o. home page at:
http://ppublishing.org.

Material disclaimer

The opinions expressed in the conference proceedings do not necessarily reflect those of the Premier Publishing s.r.o., the editor, the editorial board, or the organization to which the authors are affiliated.

Premier Publishing s.r.o. is not responsible for the stylistic content of the article. The responsibility for the stylistic content lies on an author of an article.

Included to the open access repositories:

ULRICHSWEB™ GLOBAL SERIALS DIRECTORY

Typeset in Berling by Ziegler Buchdruckerei, Linz, Austria.
Printed by Premier Publishing s.r.o., Vienna, Austria on acid-free paper.

Section 1. Architecture

https://doi.org/10.29013/AJT-19-11.12-3-6

Kosmii Mykhailo Mykhailovych,
Candidate of Law, Associate Professor, Dean
King Danylo University
E-mail: kosmiy.lud@gmail.com

INTANGIBLE FACTORS OF IMPACT ON SHAPING THE SMART CITY

Abstract. The article deals with the main factors of impact of intangible factors (legislative, mental and ethical, historical and cultural, religious and spiritual, aesthetical and landscape-related, etc.) on the spatial structure of the modern city. It defines the prospects of organizing a modern Smart City.

Keywords: intangible, spatial structure, urban development space, Smart City.

Creation and development of cities from the ancient times to the present are an evidence of the activity of human culture, a sign of the capacity of society for organized forms of life. Cities were not only unique elements of specific civilizations, they created a separate spiritual world within the limits of their own spatial organization.

Modern discussions about the forms of organization of cities are quite justified, and their severity is explained by the lack of scientific approaches to the search for the meaning of city's existence. This is important because, over the years, the cities have acquired not only material but also intangible image. They have evolved into unique functional, historical, cultural and spiritual centers. The material dimension of spatial organization of the city is realized through the study of buildings, structures, streets, squares, planning and communication systems, etc., which are considered as key elements. But each of these elements has its own soul, character, age, beauty, energy of communication as well as carries information, forms a microclimate, provides connections with the outside world, types of reactions to external influences, as well as a spiritual dimension, namely the psyche, the memory of space, continuity, genius and uniqueness.

Modern cities feel the dominant influence of information systems, new technologies, ideas of universalism and cosmopolitanism. According to this, a foundational concept of urban development for the last decade is the idea of creating the Smart City. The general theoretical and practical foundations of Smart City organization were developed by renowned scientists: M. Eremia, L. Toma, M. Sanduleac [2], I. Zubizarreta, A. Seravalli, S. Arrizabalaga [39], S. Joss, F. Sengers, D. Schraven, F. Caprotti, Youri Dayot [5] and others. Such an interest is natural because people have always been interested in the issue of an ideally organized space, and modern technological advances have brought us closer to the satisfaction of this desire.

In general, the Smart City concept considers informational, technical, technological and communication aspects of spatial structure organization. In this concept, the city encourages people to behave appropriately and helps them to make rational decisions. "Smart City" is better prepared for solving the problems and responds to the tasks and challenges of

today more quickly. Technology and decisions about this city are aimed at managing the city itself, its transportation system, energy use, health care, water use and waste disposal, etc. effectively. However, the concept also raises criticism, in particular: a) the threat of neglect of not information and technological, but also important components of urban development; b) the need for processing databalk; c) the focus of the model on business and functional rationality.

In order to avoid these negative factors, it is worth learning possible consequences of impact of intangible factors (legislative, mental and ethical, historical and cultural, religious and spiritual, aesthetical and landscape-related, etc.) on the urban development space, which allows to form an integral concept of the Smart City.

Actually, the urban development space is considered in the architecture in a narrow and wide meaning. One of the first researchers, who formed an integral understanding of urban development space, was O. Hutnov who suggested viewing the urban development space as the urban development system with the following components: construction structure (filled with a variety of spatially localized functions); communicative carcass (the chain of roads of different categories and their intersections — junctions); social activity centers (areas of junctions of transport communicative carcass filled with the functions of public service); engineering support network; landscape and ecology carcass (open green spaces connected with the natural base of the city). Nowadays, it is traditional to differentiate the urban development space and the urban development system. The first is considered as "the multi-vector space of human, natural, functional and temporal characteristics which houses a life cycle of urban development systems", the second one — as "a complex dynamic system which consists of a combination of inhabited places, connections and attitudes in a multidimensional natural, social and economic space".

All these definitions clearly suit the conception of the Smart City, since construction structure, communicative carcass, social activity centers, engineering support network, landscape and ecology carcass can be systematized using specific legal framework, following mental and ethical, historical and cultural, religious and spiritual, aesthetical and landscape-related basis. Modern IT allow monitoring all changes of above-mentioned factors and effectively make amendments to the urban development legislation.

In our opinion, at first it is useful to consider demands of inner world of a person within the process of organization of the Smart City. Nevertheless, the category of "space" is philosophical and it acts as a primary basis of organization of existence. Studying the urban development space allows understanding those factors, which are important for developing and organization of the Smart City in the 21st century.

The first doctrine of space was formed by Newton and Democritus. However, M. Heidegger rightly noted that the relation of man to the world is spatial. In this case, space is a place for human interaction with the outside world and cannot have strong territorial boundaries, because each person defines the framework of his interaction. There are times when the framework of human and environment interaction is clearly defined and limited. Therefore, we cannot speak of the spatial relation of man to the world around him. In this case, it is advisable to apply the notion of "structure", which is primary to architecture. What is most interesting is that the intangible affects both the development of "space" and "structure" in architecture and urban development. Since space is a neutral, remote and emotionless environment for human life [8, c. 86], it cannot develop and exist without the influence of spirituality, morality, various worldview imperatives formed by an individual or a group of people. They are difficult to measure, to determine, but anthropogenic impact on urban development space is extremely important. Similarly, the "environment" reflecting the spiritual and effective state of a person as a creator of urban development space cannot develop solely under the

influence of material factors. This can lead to a loss of spiritual component.

The study of urban development space in the context of the impact of intangible is important in view of the fact that during all the historical stages of urban development, we observe the active involvement of residents in the design process. This has allowed people to participate directly in the improvement of public space, which is an important component of urban development space. Urban development space is a broad concept that is based on the understanding of space as a place of residence of a person and the focus of his social and everyday needs, and therefore, the transformation of space as a place for everyone into space for everyone occurs in the moment of the person's impact on the design of urban development space.

On the other hand, not every urban space is suitable for creativity because it also should be organized considering to potential of that "creative stratum of population" that will change it. Such formulation leads to the situation, where there is a chance for development of a place, where there is an active group of population that is ready to change the space around itself. This group is laying the potential and forming the basis for changing the urban space from only the residence into the place of development too. Perfectly organized urban development space is a precondition for further development of a city. Another important component in the process of such transformation of the city is a value system which begins to dominate in the urban development and to determine the strategies of urban development. The main value of the urban development culture of creation has always been a possibility of self-realization.

As a conclusion, it should noted that the main task is formation of clear norms of law which not only guarantee meeting human needs, but also formation of clear limits of their participation in the process of development and building of the city. A person can form comfortable living environment independently. Harmonious development of the city requires the application of information technologies as well. The most interesting thing is that it is possible to establish a relationship between the regulatory acts, human needs, moral and ethical factors and modern informational technologies through a clear understanding that the spatial structure of the city is affected by not only material but also by intangible factors.

In our opinion, intangible is much more important, it forms the image of the city, defines its history which displays the interrelations between the society, the memory, the science, the art, and so on. The image of the city creates, first of all, spiritual and scientific life providing it with cultural, artistic and intellectual state, forming the quality level of human dimension — aspirations and needs of the residents, culture and art, consciousness and language. A separate aspect of intangible is the formation of legal norms, which, on the one hand, are a regulator of the city development, and on the other hand, they embody the historically shaped customary rules and principles of interaction of human collectives. The importance of intangible component is explained by the fact that in the last centuries it has turned into a required attribute of the development of spatial organization of the city, therefore, the content of the regulatory acts has to satisfy not only the needs of society, but also practical aspects of spatial organization while taking into account the anthropological, economical, moral and spiritual factors.

References:

1. Dahinden J. Mensch und Raum. Man and Space. International Symposium on Architecture. – Wien, 1984.
2. Eremia M., Toma L., Sanduleac M. The Smart City Concept in the 21st Century. Procedia Engineering. – Vol. 181. 2017. – P. 12–19. URL:https://doi.org/10.1016/j.proeng.2017.02.357.

3. Gutnov A. E. Evolyutsiya gradostroitel'stva. – M.: Stroiizdat, 1984. – 256 p.
4. Habrel M. M. Metody ekspertnoi otsinky prostorovoi orhanizatsii mistobudivnykh system. Mistobuduvannia ta terytorialne planuvannia: Nauk.-tekhn. zbirnyk. – K.: KNUBA, 2002. – Vyp. 11. – P. 14–23.
5. Joss S., Sengers F., Schraven D., Caprotti F. Youri Dayot The Smart City as Global Discourse: Storylines and Critical Junctures across 27 Cities. Journal of Urban Technology. – Vol. 26. 2019. URL:https://doi.org/10.1080/10630732.2018.1558387.
6. Kozlova L. V. Opyt Germanii v transformatsii obshchestvennykh prostranstv mikroraionov 1960–80-kh gg. Gradostroitel'stvo i urbanistika, 2017. – No. 2. – P. 255–267. URL:https://marhi.ru/AMIT/2017/2kvart17/PDF/20_AMIT_39_KOZLOVA_PDF.pdf.
7. Moiseev Yu. M. Porogi neopredelennosti v sisteme gradostroitel'nogo planirovaniya: dissertatsiya … doktora arkhitektury: 05.23.22. Mesto zashchity: FGBOU VPO Moskovskii arkhitekturnyi institut (gosudarstvennaya akademiya), 2017. – 345p.
8. Rochniak Yu. A. Arkhitekturnyi prostir i arkhitekturne seredovyshche: poshuk vidpovidei. URL:http://ena.lp.edu.ua:8080/bitstream/ntb/36747/1/14_84–87.pdf.
9. Zubizarreta I., Seravalli A., Arrizabalaga S. Smart City Concept: What It Is and What It Should Be. Journal of Urban Planning and Development. – No. 142(1):04015005.·– May, 2015. DOI: 10.1061/(ASCE)UP.1943–5444.0000282.

Section 2. Information technology

https://doi.org/10.29013/AJT-19-11.12-7-14

Dolhikh Anastasiia Olekhivna,
postgraduate student, the Faculty of Applied Math
Dnipro National University named after Oles Honchar,
E-mail: dolgih.nastya@gmail.com

Baybuz Oleg Grigorovich,
Doctor of Technical Sciences, Professor,
Dnipro National University named after Oles Honchar,
Head of The Department of Mathematical Support
of Calculating Machines, the Faculty of Applied Math
E-mail: obaybuz@ua.fm

THE SOFTWARE TECHNOLOGY OF TIME SERIES OUTLIERS' IDENTIFICATION

Abstract. The article analyzes the modern methods of time series outliers' identification. A new model of anomalous values detection has been introduced. Results of the proposed model work have been presented.

Keywords: time series, outliers, adaptive models, residuals, interquartile criterion.

1. Introduction

An outlier is a value that is significantly distant from other similar points. There are two reasons why these values need to be correctly identified. Firstly, their emergence may indicate an atypical state of the process under study. For example, in the financial sector, timely identification of outliers is necessary to track bank fraud attempts, detect unusual credit card transactions, or case of card theft [7]. The second reason for the importance of conducting the outliers' detection procedure is that the emergence of such values can significantly affect the performance of the built model, which causes a decrease in the accuracy of future time series values forecasting [7–8]. The current work is devoted to the development of a procedure for identifying anomalous time series values that allows not only to find outliers but also to determine their type. The article presents the result of the proposed method on series of financial indicators.

2. Analysis of recent research

According to the IBM Knowledge Center resource [9], at least six types of time series outliers are distinguished nowadays. The most important from a business standpoint are the following:

1. Additive outlier, or AO (additive outlier) – an unexpected large or small value, which is very different from the other levels of the series (Fig. 1). They appear once and have no effect on other values [10].

2. Temporal changes, or TC (temporal changes), occur when large or small values, uncharacteristic for the time series dynamics, appear over a short period of time (Fig. 2) [10].

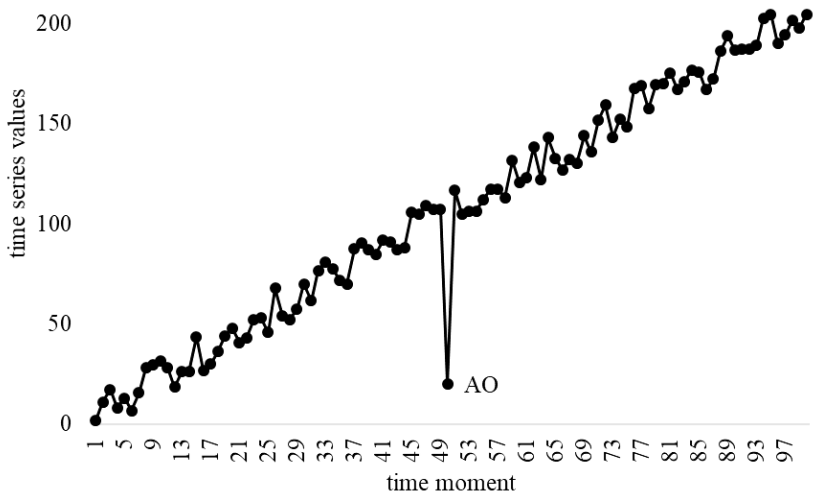

Figure 1. Additive outlier

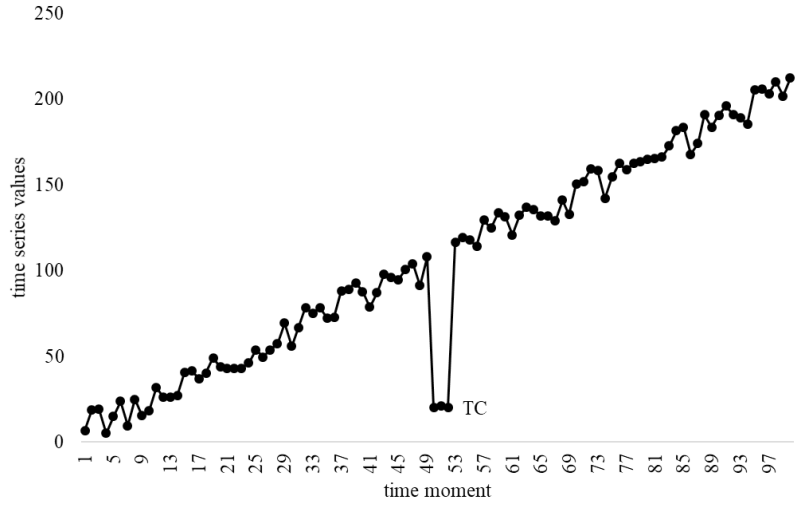

Figure 2. Temporary changes

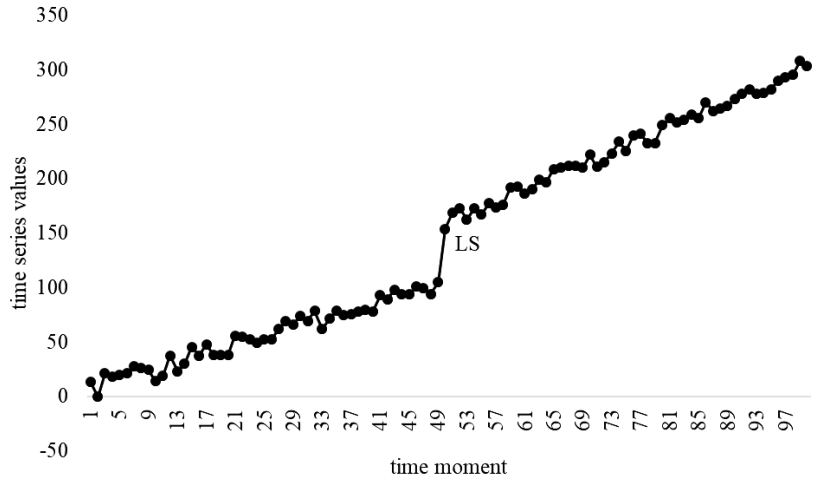

Figure 3. Level shift

2. Shift of level, or LS (level shift) – sharp change of levels of a series. All the observations that occur after this kind of outlier move to a new level (Fig. 3).

Having analyzed the latest researches in the field of time series analysis, one can conclude that anomalies detection methods can be divided into three groups.

The first group includes statistical approaches based on standard deviation [12]. They are used to detect outliers in a sample of random numbers. However, the use of such approaches for the time series analysis often does not produce the desired results, since the time series have significant differences from the samples [1]. A better solution is to identify outliers using the Irwin method [11]. Its main idea is not to compare directly the series levels but to explore the differences between the current series values and the previous ones. The criterion is easy to understand and implement. However, according to the work [11], this approach makes it impossible to correctly identify two outliers going successively, one after another, and to distinguish the "normal" value following immediately after anomalous one, from the outlier.

The second group introduces methods that use algorithms of data classification, such as decision trees and neural networks, to search for time series outliers [10]. Obviously, with this approach, it is necessary to have a training sequence, previously divided into two classes: "anomalies" and "usual values", which significantly restricts the possibilities of this group methods applying.

The third group consists of methods that attempt to reproduce the most plausible model of the input time series and to identify outliers not in the original sequence but in the series of residuals. The methods of this group show quality results and are ones of the most applicable nowadays. The algorithm proposed by American researchers in the work [2] has become widespread. Its implementation is available in the *tsoutliers* library of the well-known statistical data processing package *R* [6]. The main idea of this method is to build mostly corresponding to the input time series *ARIMA(p, q, d)* model and, after that, perform outliers detection in the residuals series. In order to achieve quality results, it is necessary to find the optimal values of the auto-regression order, *p,* integration order, *d,* and the moving average order, *q*. According to the authors [4], the number of models that need to be built and evaluated with this approach can reach 488. This could take a long time, especially when it comes to big flows of input data.

Based on the performed analysis, it could be concluded that a promising area of research is the development of more "faster" models of outliers' identification. A topical issue is to consider the use of adaptive forecasting methods to interpolate time series values. They do not require a larger number of parameters to be calculated, while displaying qualitative forecasting results.

3. Setting of the problem

To develop the procedure of time series outliers' identification based on adaptive forecasting models the following tasks have been solved:

– implement adaptive models of time series forecasting;

– develop a model for anomalous values detection in the series of residuals;

– develop an algorithm for the abnormal value type determination ("AO", "TC", or "LS");

– evaluate the quality of the proposed model on the time series of financial indicators.

4. A new procedure of time series outliers' identification

To construct the optimal time series model adaptive forecasting methods have been used. Despite the simplicity of the implementation, they show quality results [3, 14]. For training adaptive models, a genetic algorithm with real encoding has been used [3]. Once the optimal model of the original time series has been found, anomalies identification procedure in the residuals time series can be executed. Below is the detailed description of the proposed approach.

1. Calculate the predicted values of the time series $\{\widehat{u}_t\}$.

2. Calculate the series of residuals $\{e_t\}$, $e_t = u_t - \hat{u}_t$.

3. Perform the identification of residuals time series outliers. To do this the interquartile distance procedure has been used [5]. Unlike other statistical criteria of the outliers' search, its use does not require analyzed data to be normally distributed. This is an important factor, since this condition is rarely met in real financial analysis tasks. On the first iteration of the algorithm as an adjusting coefficient, $\mathrm{Coefficient}$, in the interquartile distance procedure the value 3 is applied. This value is usually used to find the outer boundaries of the data set. All values that are outside the limits of the set are considered as significant outliers. On the further iterations of the algorithm, this value has to be updated.

4. Determine the type of found outliers: "AO", "TC" or "LS". To do this, the length of abnormal values sequence to which the current outlier is included, $\mathrm{outliers\_length}$, has to be calculated. If $\mathrm{outliers\_length} = 1$, then the type of this outlier is "AO". If $1 < \mathrm{outliers\_length} < \mathrm{threshold}$, that means that we are dealing with the "TC" outlier type. Otherwise, if both of the above conditions are not executed, then the type of the found outlier is "LS". As the threshold value, $\mathrm{threshold} = 0.02 \cdot \mathrm{N}$ is used, where N is the length of the original time series.

5. After the types of all found outliers are determined, outliers of the input series need to be replaced by the predicted values of the constructed model.

6. Reduce the outer limits of the data set using the following formula:

$$\mathrm{Coefficient} = \mathrm{Coefficient} \cdot (1 - \mathrm{reduce}),$$

$$\mathrm{reduce} = 0.14813$$

7. If the iteration number has reached the maximum allowed value, $\mathrm{MAX\_ITER}$, or the new outliers have not been found at the current iteration, the algorithm is terminated. Otherwise, repeat the outliers detection procedure from step 1, but at this point adjusted time series (e.g. time series received at the fifth step) has to be used as the input series.

By default, the maximum number of iterations $\mathrm{MAX\_ITER}$ equals three. It has been empirically found that reducing this value leads to the fact that the program cannot find all the important anomalies, while increasing – causes too many time series levels detection as outliers, even the values that completely correspond to the process dynamics.

5. The results of the proposed method of the outliers' detection

This section summarizes the results of the proposed model testing on the financial time series.

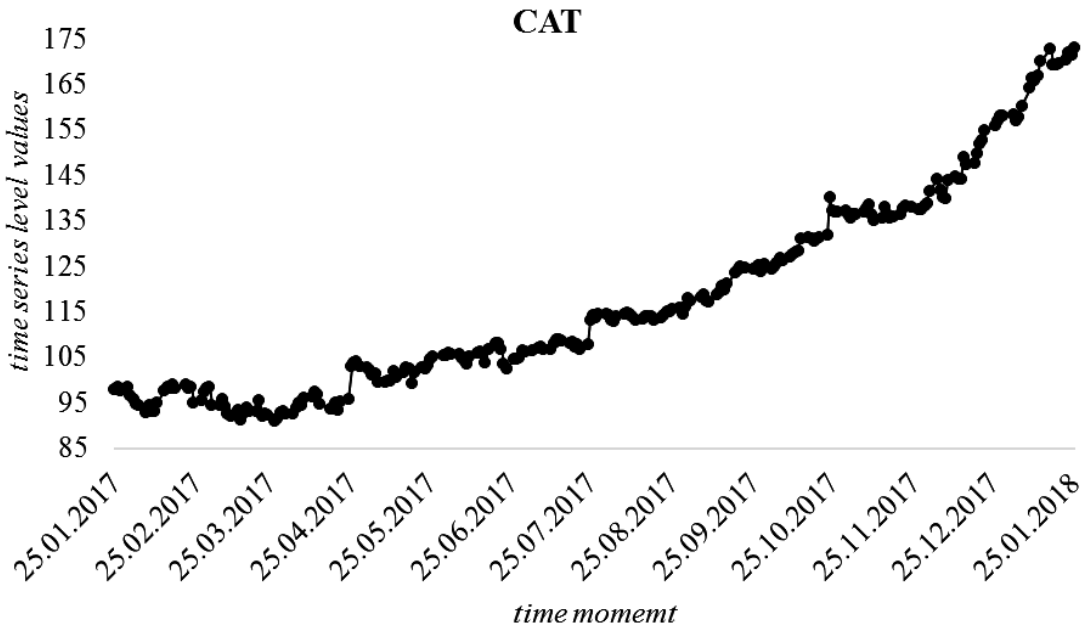

Figure 4. CAT time series

The (Fig. 4) shows the open prices of Caterpillar Inc. stocks in the period of time from January 2017 to January 2018. Data have been downloaded from "Yahoo! Finance" resource [13] (Fig. 4).

During the time series preliminary analysis, the Spearman test for the trend presence and the serial correlation test for the periodic component existence have been conducted. According to their results, there is a trend component in the series and there is no pronounced seasonality or autooscillations.

To interpolate time series level values Taylor-Wage adaptive model has been used. Fig. 5 shows the time series of residuals.

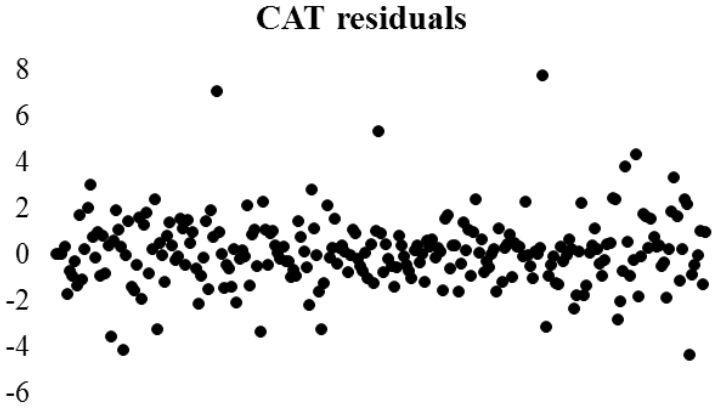

Figure 5. A series of residuals

Having analyzed the diagram 5, one can conclude that the series of residuals is stationary, the values average fluctuates near zero, residuals look like random numbers independent on time point. These considerations have been confirmed by the performed statistical tests. One-sample Student's test has been used to test the equality of mean to zero. The trend absence has been confirmed with using the Spearman test for the randomnicity. An important step in analyzing the model's residuals is to check the absence of autocorrelation between them. To do this Darbin-Watson test has been applied. The results showed that there was no interdependence between the levels of the series. In our case, such properties of residuals are important not only because they confirm the quality of the built model, but also because the residuals series is used for anomalies identification.

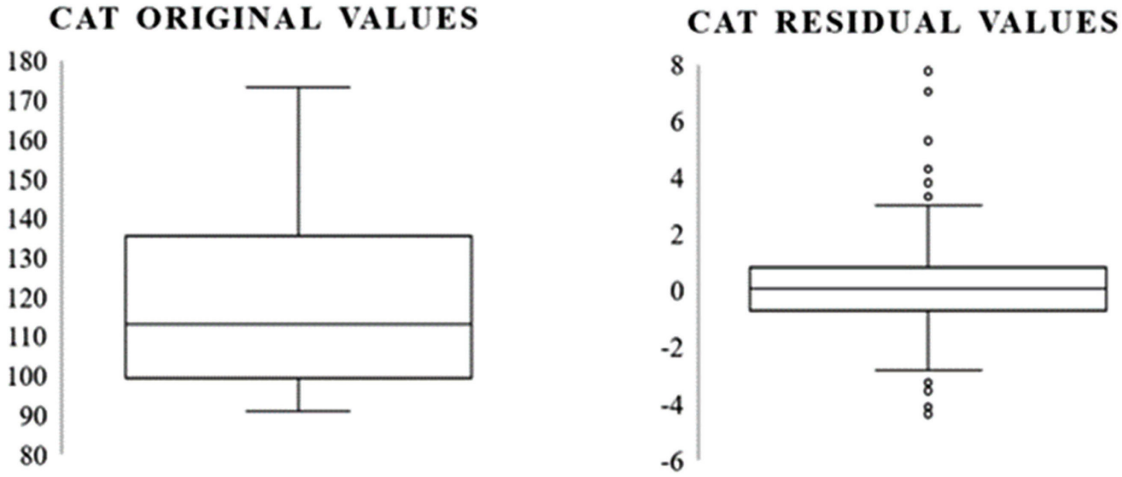

a) b)

Figure 6. Box-plot diagram of the original series (a) and residuals series (b)

Table 1. List of CAT series outliers

No.	Series level number	Series level value	Outlier type
1.	63	102.88	LS
2.	126	113.24	LS
3.	190	140.06	TC
4.	226	148.85	AO

As one can see from the Box-whisker plot graphs (Fig. 6), anomalous values cannot be detected in the original series values. However, after transition to residuals series "applicants" to outliers can be easily distinguished. In (Fig. 6 b) they are shown as black dots outside the outer limits of the data set.

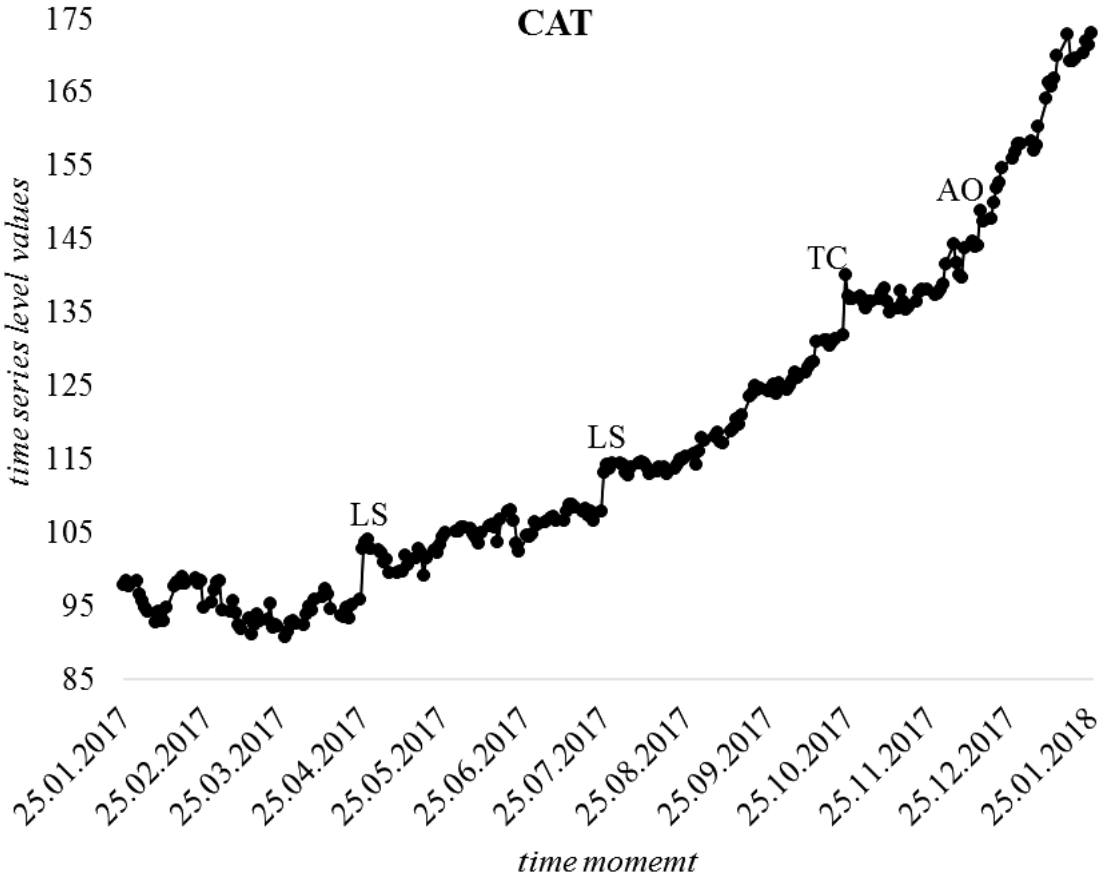

Figure 7. CAT time series with outliers

Table 1 and Fig. 7 show the results of the proposed outliers' identification procedure application to the CAT time series.

The proposed anomaly identification procedure revealed four anomalous values. The first two outliers are of the "LS" type. The third one has been identified by the procedure as the "TC" outlier because it covers only a few values. The last anomalous value is single one and doesn't have any effect on the future values of the series, so its type is defined as "AO". The procedure *tso* of the package R [6] shows similar results.

Table 2 summarizes the results of comparing the time costs required to perform the proposed procedure and the *tso* function of the *tsoutliers* library of R package [6] on the series that represent stock prices of well-known American companies from 2017 to 2018.

Table 2. – Time costs required to detect outliers with using adaptive models and ARIMA-models based approaches

No.	Time series	Procedure based on adaptive models, ms	Procedure tso from library of tsoutliers package R, ms
1.	AAON	0.379	0.405
2.	CAT	0.726	1.122
3.	DBD	0.372	2.025
4.	MSFT	0.44	0.686
5.	CSCO	0.317	0.379
6.	BGS	0.623	6.556
7.	IBM	0.694	0.47
8.	ABC	0.656	3.108
9.	BK	0.529	0.388
10.	CAKE	0.521	7.147

Having analyzed Table 2, one can conclude that the use of the procedure proposed in the article for most time series allows to reduce the time required to identify anomalous values, with the exception of only IBM and BK time series.

6. Conclusions

During the study, a new procedure of time series outliers' identification has been developed. Its advantage over many other approaches is that it not only detect anomalies, but also determines their type. The scientific novelty of the proposed method is that it uses adaptive forecasting models to interpolate the series values and the interquartile distance criterion to detect for outliers in it. Proposed procedure allows correctly identify a large number of anomalous values and reduce the time required to do this. Prospects for further research are testing the feasibility of the proposed approach usage in the big data analysis.

References:

1. Biloborodko O. I., Yemelyanenko T. G. Dynamic Series Analysis. Dnipro: Dnipro national university named after Oles Honchar, 2014.– 80 p.
2. Chen C., Liu L. Joint Estimation of Model Parameters and Outlier Effects in Time Series. Journal of the American Statistical Association. 1993.– Vol. 88.– P. 284–297.
3. Dolhikh A. O., Biloborodko O. I., Baybuz O. G. Finding the optimum values of adaptive models parameters for time series forecasting using genetic algorithm. Actual problems of automation and informational technologies. 2016.– Vol. 20.– P. 11–22.
4. Hyndman R. J., Khandakar Y. Automatic time series forecasting: The forecast package for R. Journal of Statistical Software. 2008.– Vol. 26.– No 3.
5. Inter-quartile range, outliers, boxplots. URL:https://www.sfu.ca/~jackd/Stat203_2011/Wk02_1_Full.pdf
6. Javier López-de-Lacalle. Detection of Outliers in Time Series. Package 'tsoutliers'. 2019. URL: https://cran.r-project.org/web/packages/tsoutliers/tsoutliers.pdf (application date: 06.12.2019)
7. Mab Alam. Outlier detection with time-series data mining. Data Science Central – The online resource for big data practitioners. 2018. URL:https://www.datasciencecentral.com/profiles/blogs/outlier-detection-with-time-series-data-mining (application date: 06.12.2019)
8. Nosov S. S., Belovodsky V. N. Pleliminary processing of meteo time series: methods, experiments, results. Informatics and computer technologies. 2011. URL:http://ea.donntu.edu.ua/bitstream/123456789/12

786/1/%D0%9D%D0%BE%D1%81%D0%BE%D0%B2%20%D0%A1.%D0%A1.%20.pdf (application date: 06.12.2019)
9. Outliers. IBM Knowledge Center. URL:https://www.ibm.com/support/knowledgecenter/en/SS-3RA7_15.0.0/com.ibm.spss.modeler.help/ts_outliers_overview.htm (application date: 06.12.2019)
10. Pavel Tiunov. Time Series Anomaly Detection Algorithms. Stats and Bots. URL:https://blog.statsbot.co/time-series-anomaly-detection-algorithms-1cef5519aef2 https://blog.statsbot.co/time-series-anomaly-detection-algorithms-1cef5519aef2 (application date: 06.12.2019)
11. Trofimenko S., Marshalov A., Grib N., Kolodeznikov I. Modification of the Irwin method for the detection of abnormal levels of time series: methodology and numerical experiments. Modern problems of science and education. 2014.– Vol. 5.
12. Will Badr. 5 Ways to Detect Outliers/Anomalies That Every Data Scientist Should Know (Python Code). Towards Data Science. URL:https://towardsdatascience.com/5-ways-to-detect-outliers-that-every-data-scientist-should-know-python-code-70a54335a623 (application date: 06.12.2019)
13. Yahoo! Finance. URL:https://finance.yahoo.com/ (application date: 21.04.2019)
14. Yu. P. Lukashin. Adaptive methods for short-term time series forecasting.– M., 2003.– 416 p.

Section 3. Technical sciences

https://doi.org/10.29013/AJT-19-11.12-15-19

Mambetsheripova Ajargul Abduganiyevna,
(PhD), senior teacher, the Faculty industrial-technology
Karakalpak State University named after Berdaq
E-mail: majargul@bk.ru

MODERNIZATION OF THE TECHNOLOGICAL PROCESS OF A CENTRIFUGAL DISK APPARATUS FOR APPLYING MINERAL FERTILIZERS AND SUBSTANTIATION OF PARAMETERS

Abstract. In article are brought information about the design, the technological process of new pneumo -centrifugal apparatus for application of mineral fertilizers and their mixtures, as well as the results and analysis of theoretical researches, in particular, the radius of fertilizer supply to apparatus.

Keywords: Centrifugal apparatus, mineral fertilizers, construction, technological process, windage, radius.

Introduction

Production of technical facilities and technology for distribution of mineral fertilizers across surface of the field in a uniform and a predetermined amount of the distribution is the key to increasing use of fertilizers in the world. "Given that about 60% of all worldwide mineral fertilizers are sprayed on the field," development of high-quality fertilizer machines and apparatus is an important task [1]. At the same time, much attention is paid to improving the constructive scheme of fertilizer machines and substantiating the technological process, improving quality of work during the interaction of working parts with mineral fertilizers and their environmental movement.

Related work and dl scussi on

It is known that scattering technological process of mineral fertilizers fertilizer hopper sole poured through holes in centrifugal devices. Speed of mineral fertilizers poured into the centrifugal apparatus from bunker hole [2],

$$V_T = \sqrt{2gh} \quad (1)$$

where g – is acceleration of free fall, m/s²; h – height of fertilizer spillage, m.

Given that distance between bottom of the bunker hole and apparatus is h = 0.03–0.05 m, the spill rate of fertilizer grains of different sizes and shapes can be assumed to be the same.

Mineral fertilizers, grains of specified distance and the speed and angle of throw, they received disk depends on distance r_0 (Figure 1). When determining distance r_0, it is important to note that the friction force of centrifugal force $m\omega^2 \cos\psi$ acting on mineral fertilizer grains is greater than that of $f\ m\omega^2 \cos\psi$. When this condition is met, fertilizer grains move across the spade to its edge.

In this context, r_0 is minimum value of distance [3],

$$r_{0\min} \geq R\sqrt{1+f^2}\ \sin\psi \quad (2)$$

where R – is the radius of centrifugal disk, m; f – coefficient of friction mineral fertilizer on shovel; ψ – angle between the tangent and radius vector to the

point where the fertilizer grain meets the shovel, degrees. (2) expression $R = 0.30; f = 0.5$ and $\psi = 35^{\circ} - 40^{\circ}$ when calculated by the values are $r_o = 0.034–0.066$ m. (2) The calculation scheme of expression is shown in Figure 1, as well as provision of condition

$$m\omega^2 r_0 \cos\psi \geq mf\omega^2 r_0 \cos\psi \qquad (3)$$

Using mathematical operations and taking coefficient of friction in the range $f = 0.35–0.5$, expression (3) was achieved. Analysis of expression (3) showed that the value of centrifugal force is 2.0–2.2 times greater than the value of frictional force generated.

Hole opening in the bottom of bunker location in relation to the working surface and shovels of centrifugal disk affect the values of fertilizers outlet and scattering corners.

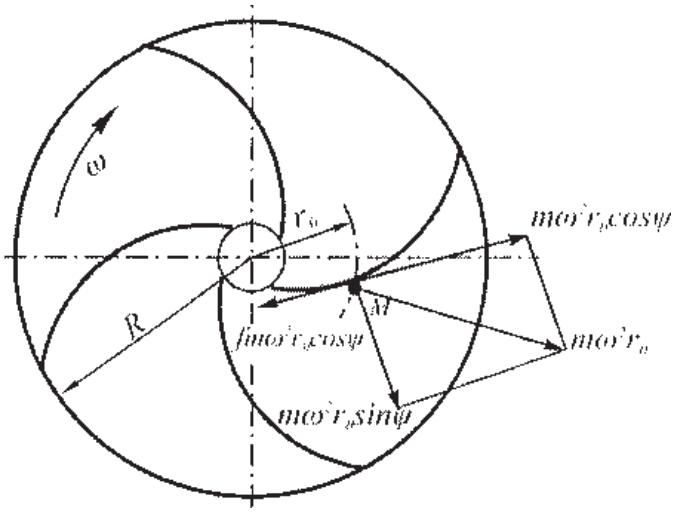

Figure 1. r_0 scheme of distance determination

Academician P. M. Vasilenko detailed the movements and equations of mineral fertilizer grains in system of different coordinates on shovels with different shapes [4].

As is known, shovels are mounted in the radial direction on disk in centrifugal devices of existing fertilizer machines. Installation of shovels in this way poses constructive problem with installation of additional air bubbles under each of them. This is because the absolute velocity direction of fertilizer grains is inconsistent with direction of additional airflow, which means that the process of technological operation of apparatus is not fulfilled. Taking into account the foregoing, shovels in the form of logarithmic spirals were selected (Figure l).

Methodology

A worldwide literature review known that of centrifugal discs' production with a diameter of 400–700 mm. Disk centrifugal apparatus with diameter of 400–500 mm are usually installed in two fertilizers per machine. Disk apparatus with diameter of 600–700 mm are mounted on each fertilizer machine one piece [5].

Based on the above and size of fields on farms of the Republic, we also received 600 mm diameter disk centrifugal apparatus and decided to install one fertilizer machine.

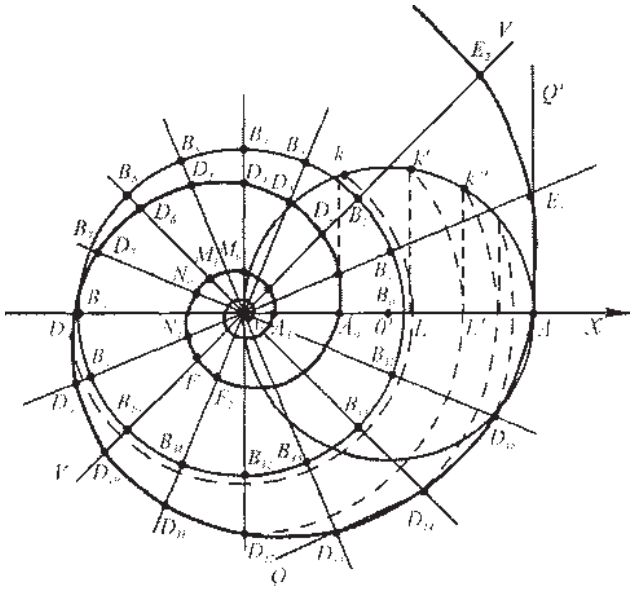

Figure 3. Logaritrmic spiral

It is widely used in centrifugal apparatus that the number of shovels is four and that they are placed symmetrically on disk surface. This is because the apparatus disk is balanced with large number of rotations and requires reliability for safety reasons. However, there are differences in the shape of shovels and their adjustment to the disk radius. The basis of this diversity lies in the way technology is implemented. In particular, shape of the shovels is chosen as packing form to reduce friction force during the movement of fertilizer grains through shovels [6], It is well known that the spirals are logarithmic, archaemidic, and hyperbolic (Fig. 2).

In a logarithmic spiral, the angle between the tangent point and the radius vector held at each point is constant. In this case, it is possible to select any part of logarithmic spiral with a central angle of 90 °.

When constructing logarithmic spiral and selecting required section, position of radius-vector length is equal 'to the radius of centrifugal disc and corresponding branch OA_0D_4.

When constructing logarithmic spiral and selecting required section of radius- vector length centrifugal disc that is equal to the radius *R* and corresponding piece of OA_0D_4 were selected.

Experimental results

Relative and displacement velocities of mineral fertilizer grains calculated for shovel in form of logarithmic spiral, used their vector sum to give absolute velocity, and determined absolute velocity direction of fertilizer grains (Figure 3).

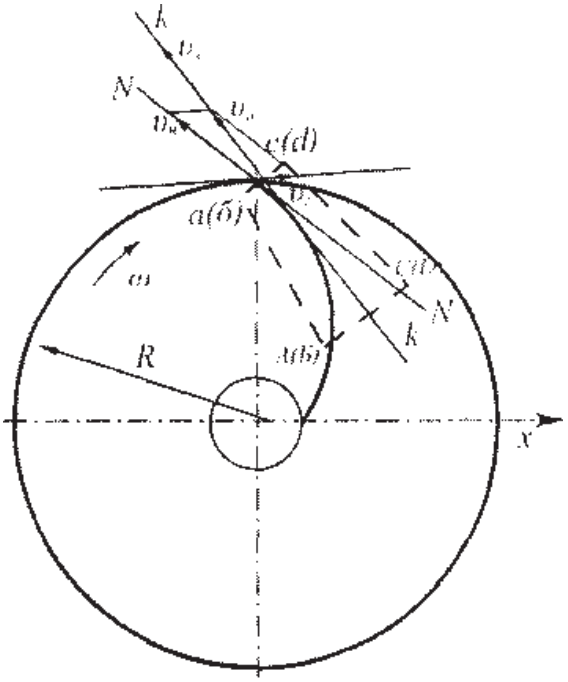

Figure 3. Scheme for selecting additional airflow direction by adjusting the absolute velocity of fertilizer grain

Determining absolute velocity direction shown in Figure 3 and corresponding additional airflow diagram allow determine position of device to generate additional airflow. It is required to select the direction of additional airflow produced in such a way that it is in parallel with absolute velocity of fertilizer grains. Only then will use of additional airflow be more effective. To achieve this, the K.K line at the absolute speed of fertilizer grains throwing is passed through the bottom of disc. The line AD is perpendicular to KK. The AD line length is selected based on disk diameter. In this case, 0.15 m was selected. We will pass parallel ad line to AD from the logarithmic spiral shovel of disc at the point where it ends, and obtain a length of 0.05 m. Then AD: ad=3. The resulting AadD shaped trapeze is schematic view of device that generates additional airflow.

Given that fertilizer grains thrown from centrifugal disk in horizontal plane, we direct additional airflow and velocity vector along the horizontal plane. To do this, disk edge of base taken parallel to the disk plane. This condition was achieved by selecting the height access point of device 0.10 m. Accordingly, height of outlet hole was selected at 0.03 m. Based on the analysis and analysis of constructive technical solutions, access hole is 0.15 m wide, 0.1 m high, outlet hole is 0.05 m wide and 0.03 m high.

It has been reported in previous studies to apply of shovel in form of logarithmic spiral that convex in the direction of rotation and on short release of fertilizer grains from disk. The positive side of logarithmic spirals is that firstly, mineral fertilizer grains move with minimal friction, preventing segregation and, secondly, providing minimum value of output angle [4]. More, importantly, generated additional airflow force is parallel to tangent made to the points of shovel. This will ensure efficient use of additional air power. All of these factors provide the basis for the uniform distribution quality of mineral fertilizer grains.

Differential equation of fertilizer pieces' motion along logarithmic blade

$$\ddot{S} = \omega^2 r\cos\psi_0 - fg + f\omega^2 r\sin\psi_0 - 2f\omega\dot{S}_r \qquad (4)$$

here ψ_0 – angle, between relative velocity and the centrifugal force;

S – distance traveled along the blade, m.

Solution of equation (7)

$$S = C_1 e^{P_1 t} + C_2 e^{P_2 t} + \frac{fg\sqrt{1+a^2}}{(a+f)\omega^2} \quad (5)$$

here P_1 and P_2 – roots of equations; C_1, C_2 – initial conditions of movement, constant magnitudes $s = r_o$, $S = 0$ determined by the initial conditions of the motion when $t = 0$ (8).

Outlet angle β of fertilizer apparatus is a direct indicator that affects the uneven scattering of fertilizers. This indicator depends on fertilizer transmission distance to the disk r_o, the blade length S and angular velocity ω of disk.

The S expresses the total length of the formula (5). However, mineral fertilizers pieces are given away from the center of disk to r_o distance, not at the beginning of blade, r_1 initial radius of logarithmic spiral shaped blade (Fig. 4). As can be seen from picture $r_o > r_1$.

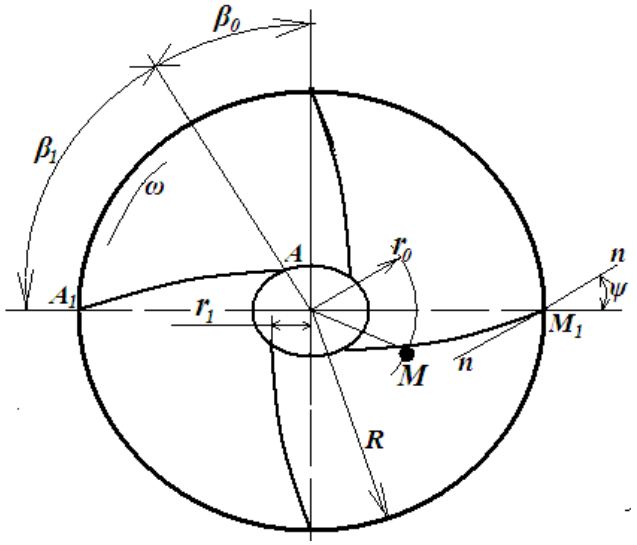

Figure 4. A scheme for determining the length of blade fertilizer grains have passed

It can be determined by the following expression of logarithmic spiral shaped blade MM_1 arc length [8]:

$$L = \frac{r_1 - r_o}{\cos\psi} \quad (6)$$

here r_1 – initial radius of blade, m;

ψ – angle, between tangential and radius vectors passing to any point.

It is shown in the line graph, influence to passed length of fertilizer grains over blade indexes in expression (7).

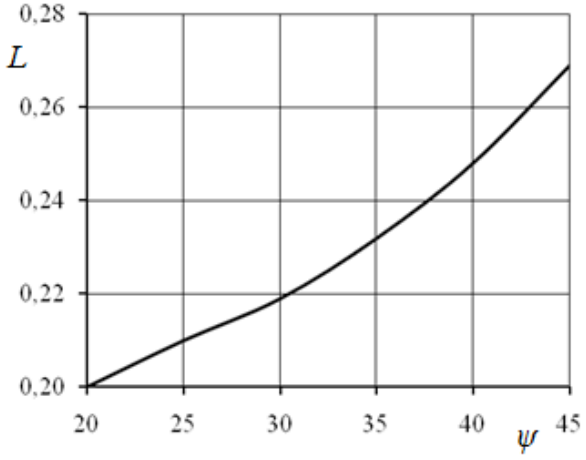

Figure 5. The line graph of change depending on angle ψ to the blade length

The graph shown in Fig.5 is constructed with radius $R = 0.3$ m, $r_1 = 0.05$ m and $r_o = 0.11$ m of disc. As shown in (Fig. 5), when the angle ψ increases, the width of blade is increasing according to with curvature regularities. The length is increasing in return decreasing logarithmic spiral of curvature radius. In this case, increased movement time of fertilizer grains by the blade. This allows the fertilizer grains to be fractionated. In this context, the length of blade is adopted 0.22–0.23 m corresponding to the angle $\psi = 30 - 35^\circ$. Fig. 5 shows a line chart of change depending on blade length r_o to fertilization distance.

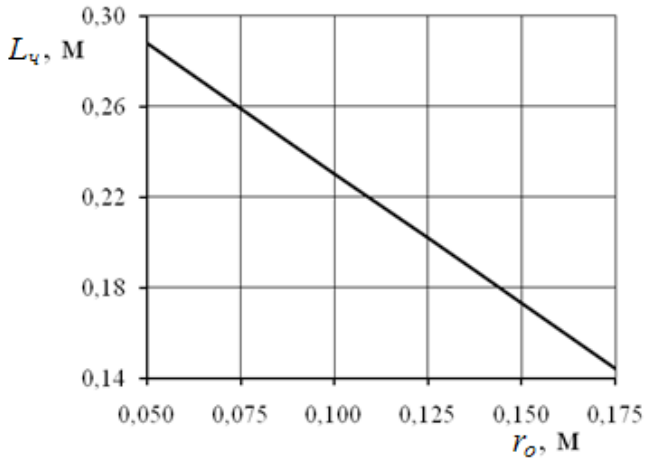

Figure 6. A line chart of change depending on blade length r_o to fertilization distance

The shown line chart in Fig.4 is constructed at a disc radius R = 0.3 m,
r_1 = 0.05 m and $\psi = 30^{\circ}$. As can be seen in (Fig. 6), fertilizer radius increases as fertilizer grains movement of blade length decreases according to the linearity law. Therefore, the radius of fertilizing is enlarged and it is close to length of disc radius. Based on the results of theoretical and experimental researches, radius of fertilizing was adopted between 0,100–0,125 m.

Conclusions

To develop the technological process of centrifugal apparatus enhances the quality of field scattering of mineral fertilizers and their mixtures with different aerodynamic properties, by mounting shovels on the top and additional airflow on the bottom.

The shovels are in the form of logarithmic spiral, with angle between the tangent and radius vector at its peripheral angles ranging between 30–35°. The proposed centrifugal apparatus is designed to simultaneously scattering the mineral fertilizers, to generate additional airflow, and redirect them after scattered fertilizing grains, blades in form of logarithmic spirals and fertilization radius will be in the range of 0.1–0.125 m.

References:

1. URL:https://www.zerno-ua.com;https://latifundist.com/spetsproekt/240-lokalno-lentochnoe-differentsirovannoe-vnesenie-udobrenij.
2. Urazboev M. Basic course in theoretical mechanics.– Tashkent: Ўқитувчи. 1966. – P. 350–358.
3. Vasilenko P. V. Fundamentals of material particles motion theory on friction surfaces in number of working bodies of agricultural machines: diss.– M., 1947.– P. 10–14.
4. Vasilenko P. M. The theory of particle motion on rough surfaces of agricultural machines.– Kiev, I960.– P. 254–256.
5. Doganavsky M. G., Kozlovsky E. V. Fertilizer machines.– M.: Mashinostroenie, 1972.– P. 272.
6. Vygodskiy M. Y. Flandbook of Higher Mathematics.– M.: Nauka, 1969.– P. 784–787.
7. Худаяров Б. М., Мамбетшерипова А. А. “Способы определения равномерности распределения минеральных удобрений центробежно-дисковыми аппаратами”. ВЕСТНИК Каракалпакского отделения Академии наук Республики Узбекистан.– Нукус, 2011.– № 4.– С. 14–16.
8. Фихтенгольц Г. М. Дифференциал ва интеграл ҳисоб курси.– Т.: Ўқувпеддавнашр, 1958.– С. 225–227.

Section 4. Transport

https://doi.org/10.29013/AJT-19-11.12-20-24

Kupelskiy Viktor,
Doctoral Student,
of the National Academy of State Border guard
Service of Ukraine named after Bohdan Khmelnitsky,
Khmelnitsky, Ukraine
E-mail: vkupelskiy@ukr.net

SOFTWARE AND ALGORITHMIC SUPPORT FOR ROAD NETWORK GRAPH LABELING IN CASE OF CHANGES IN ROAD CONDITIONS

Abstract. The article presents software and algorithmic support for labeling a graph of a road network for a continuous indeterminate case of changes in weights of edges. In order to implement the algorithm, the MATLAB programming environment was used.

Keywords: algorithm, program, traffic route, graph.

The effective solution of a significant number of applied tasks related to transportation in some cases depends on the successful choice of a traffic route. The construction of optimal routes on a labeled graph that describes a network of roads and has a certain weight of edges is a classic and thoroughly studied problem [1, 88–160]. However, in many cases, it becomes necessary to take into account the possible dynamic changes in the weight of the edges over time, which corresponds to cases of changes in road conditions. In the research [2], a technique is presented that provides the choice of optimal traffic routes for discrete stochastic, discrete determinate, and continuous indeterminate cases of changes in the weight of graph edges. In addition, using MS Visual Studio Express Edition and the C# programming language, the corresponding software and algorithmic support were developed for the discrete stochastic and discrete determinate options for changes in the weight of the graph edges. The study is incomplete as there is no software and algorithmic support for the continuous indeterminate case, and this fact defines this research.

The objective of the study is to develop software and algorithmic support for graph labeling of a road network in a continuous indeterminate case of weight changes of graph edges.

To achieve the stated objective, it is expedient, first of all, to state a problem that is adequate to the real process, to formalize it, and then to propose algorithms for solving it.

Problem statement adequate to the real process.

Let a convoy be given, which should leave the departure point (Point 1) and arrive at the destination point (Point 13). The conditions for the formation of convoy composition are similar to those specified in the research [3, 17–30]. Let also a network of roads connecting Points 1 and 2 be given. The mathematical model of a road network is a graph shown in (Figure 1).

The number of graph nodes is 13. Let it be necessary to move the convoy from Point 1 to Point 13 within a minimum period of time. To do this, it is necessary to label the graph.

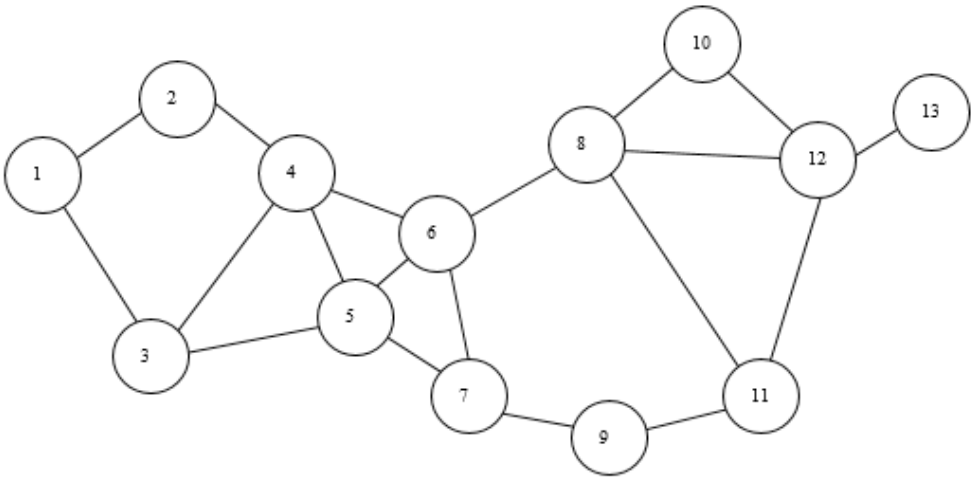

Figure 1. A graph of road network between points of departure and destination

It should be borne in mind that when moving the convoy, the movement along individual edges can be variable. This condition is determined by the influence of various conditions on the time of movement along individual edges, for example, climatic (rain, ice, fog, etc.), technogenic (blockages of the roadway, its damage due to flooding of the terrain, etc.), time changes (day, night), etc. It should be noted that we also know the distances between the graph nodes and changes in the speed of movement of all types of vehicles depending on the time of day (as an example, we use four types of vehicles), which are presented in (Tables 1, 2).

Table 1.– Distances between graph nodes

Distance (s), km																		
(1–2)	(1–3)	(2–4)	(3–4)	(3–5)	(4–5)	(4–6)	(5–6)	(5–7)	(6–7)	(6–8)	(7–9)	(8–10)	(8–11)	(8–12)	(9–11)	(10–12)	(11–12)	(12–13)
13	23	34	24	28	23	16	12	22	24	45	22	31	30	53	23	35	32	30

Table 2.– Change in vehicle movement speed during the day

Speed of individual vehicles (V_i), km/h	**Times of day (T_0), hour**																							
	00.00	**01.00**	**02.00**	**03.00**	**04.00**	**05.00**	**06.00**	**07.00**	**08.00**	**09.00**	**10.00**	**11.00**	**12.00**	**13.00**	**14.00**	**15.00**	**16.00**	**17.00**	**18.00**	**19.00**	**20.00**	**21.00**	**22.00**	**23.00**
First	51	50	50	50	53	55	60	70	80	85	90	95	95	95	90	85	80	70	60	55	55	53	52	51
Second	43	41	40	40	43	45	50	60	70	75	80	85	85	87	87	77	72	67	56	51	51	49	48	45
Third	38	37	35	35	38	40	45	55	65	70	75	80	80	82	82	75	70	62	53	47	47	44	43	40
Fourth	41	39	37	37	39	42	48	57	68	72	78	83	83	85	85	76	71	64	55	49	49	47	45	43

Statement of the main research material

We define the law of motion for each type of vehicles using spline approximation by Hermite cubic polynomials and breaking each edge into 8 interpolation nodes. The approximation results for the example of an edge (1; 2) are presented in (Figure 2).

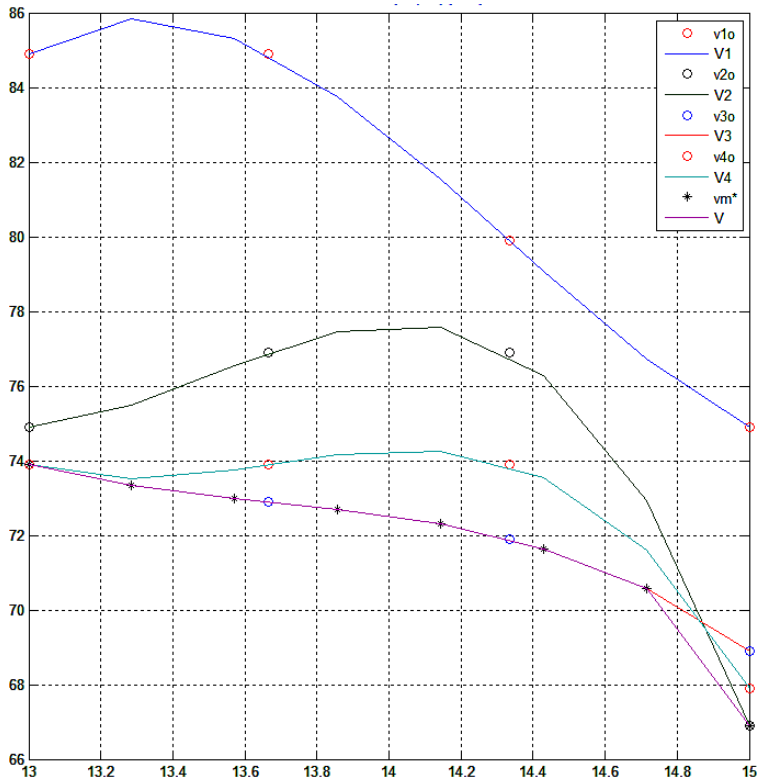

Figure 2. Speeds of all vehicle types on the edge (1; 2).

The law of speed change is determined by the formula (1) [4, 45–71]:

$$V(t) = a_k + b_k(t - t_k) + c_k(t - t_k)^2 + d_k(t - t_k)^3, \quad (1)$$

where $a_k = V(t_k)$, $b_k = V'(t_k)$,

$c_k = \dfrac{3V(t_k, t_{k+1}) - V'(t_{k+1}) - 2V'(t_k)}{t_{k+1} - t_k}$,

$d_k = \dfrac{V'(t_k) + V'(t_{k+1}) - 2V(t_k, t_{k+1})}{(t_{k+1} - t_k)^2}$ are Hermite coefficients.

We compare the speed values $V^1_{(i;j)}$, $V^2_{(i;j)}$, $V^3_{(i;j)}$, $V^4_{(i;j)}$ using the principle of minimization, which enables to find the speed of the convoy on the edge $(i;j)$, if it starts moving at the point T_0, and the results are presented in (Figure 3):

$$V_{(i;j)}(T = 0) = \min\left\{V^1_{(i;j)}(T_0), V^2_{(i;j)}(T_0), ..., V^{n-1}_{(i;j)}(T_0), V^n_{(i;j)}(T_0)\right\},$$

```
-------------------------------------------------------------------------
                Ребро ( 1 , 2 )
-------------------------------------------------------------------------
Вузли апроксимації    Час, год.     Швидкість, км/год
    k=1                 10.00           58.90
    k=2                 10.29           60.24
    k=3                 10.57           62.65
    k=4                 10.86           66.79
    k=5                 11.14           71.32
    k=6                 11.43           73.55
    k=7                 11.71           72.94
    k=8                 12.00           73.90
-------------------------------------------------------------------------
                Ребро ( 1 , 3 )
-------------------------------------------------------------------------
```

Figure 3. Speed of convoy on the edge (1;2) at $T_0 = 10$ hours

The speed value of convoy along the edge $(i;j)$ at different points in time T_0 of the start of movement, i.e. the value of the function $V_{(i;j)}(T_0 = 0)$, $V_{(i;j)}(T_0 = 1), ..., V_{(i;j)}(T_0 = 23)$, makes it possible to find the weight of the edge $(i;j)$, which may differ for different values of T_0. Using the integral approach

described in [5, 17–28], we determine the travel time along the edge $(i;j)$ using the equation:

$$\int_{t_{0i}}^{t} V_{(i;j)}(t)dt = S\left(_{i;j}\right) \quad (2)$$

or

$$\int_{t_{0i}}^{t}\left(a_k + b_k(t-t_k) + c_k(t-t_k)^2 + d_k(t-t_k)^3\right)dt = S\left(_{i;j}\right)$$

$$S_{(i;j)} = \left(a_k t + \frac{a_k}{2}\cdot(t-t_k)^2 + \frac{a_k}{3}\cdot(t-t_k)^3 + \frac{a_k}{4}\cdot(t-t_k)^4\right)\Big|_{t_{0i}}^{t}$$

Having performed the mathematical transformations, we obtain an equation of the fourth degree with respect to t (3), and the results are presented in (Figure 4):

$$p_4(t_k)\cdot t^4 + p_3(t_k)\cdot t^3 + p_2(t_k)\cdot t^2 + p_1(t_k)\cdot t + p_0(t_k) = 0, \quad (3)$$

where $p_4(t_k) = \frac{d_k}{4}$, $p_3(t_k) = \frac{c_k}{3} - d_k \cdot t_k$,

$$p_2(t_k) = \frac{b_k}{2} - c_k \cdot t_k + \frac{3}{2}\cdot d_k \cdot t_k^2,$$

$$p_1(t_k) = a_k - b_k t_k - c_k \cdot t_k^2 - d_k \cdot t_k^3,$$

$$p_0(t_k) = -S_{ij} a_k \cdot t_k - \frac{b_k}{2}\cdot t_k^2 - \frac{c_k}{3}\cdot t_k^3 + \frac{d_k}{4}\cdot t_k^4.$$

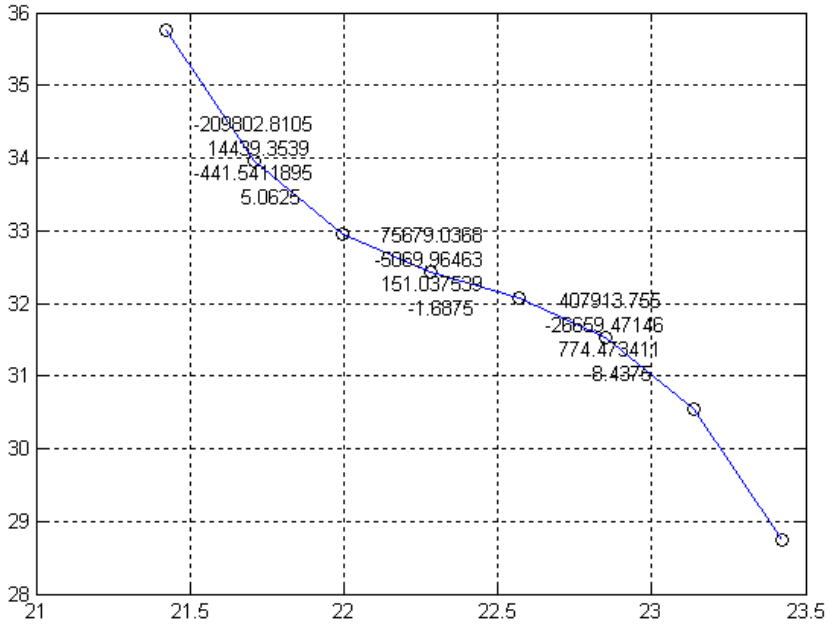

Figure 4. Values of the Hermite coefficients: $P_0(t_k), P_1(t_k), P_2(t_k), P_3(t_k), P_4(t_k)$ on edge (1; 2)

The solution of equation (3) is the time spent on the edge $(i;j)$.

After performing similar operations with all edges, we obtain a graph with the weight equal to the time spent on the move, which is defined as a function of the argument T_0:

$$a_{(i;j)} = f_{(i;j)}(T_0). \quad (4)$$

The software application is made using the programming language of the MatLab computer mathematics system. The program is implemented by a script file and two function files.

Conclusions. The developed software and algorithmic support enable to label the graph of a road network in the case of a continuous indeterminate change in the weight of edges, which takes into account the change in both the speed of movement and the hourly indicators of the beginning of movement.

References:

1. Nikolsky Yu. V., Pasechnik V. V., Shcherbina Yu. M. Discrete Mathematics.– Kiev: BHV Publishing Group, 2007.
2. Borovik O. V., Rachok R. V., Borovik L. V., Kupelskiy V. V. The method of selection of the optimal route of movement of columns of vehicles under non-stationary road network.– Zaporizhzhia: ZNTU, 2019.– No. 51.
3. Borovik O. V., Rachok R. V., Borovik L. V., Kupelskiy V. V. The mathematical model of the problem of formation of the convoy of frontier commandant rapid response and its software-algorithmic implementation.– Kyiv: MIKNU,– 2017.– No. 55.
4. Dovgyi B. P., Loveikyn A. V., Vakal Ye. S., Vakal Yu. Ye. Spline Functions and Their Use. Textbook of Taras Shevchenko National University of Kyiv.– Kyiv: KNU, 2016.
5. Borovik O. V., Kupelskiy V. V. Method of graph labelling of road network while solving the problem of selecting optimal traffic route for motor convoy of rapid mobility border command post and the algorithm of its realization.– Kyiv: MIKNU, 2018.– No. 62.

Section 5. Chemistry

https://doi.org/10.29013/AJT-19-11.12-25-28

Buronov Akrom Oydinkulovich,
Tashpulatov Khurshid Shukurovich,
Nasimov Abdullo Murodovich,
Samarkand State University, Samarkand, Uzbekistan
E-mail: xurshiduz@yandex.ru

DEVELOPMENT OF OPTICAL SENSOR FOR DISSOLVED AMMONIA WITH SOL-GEL ROUTE

Abstract. Optical sensor for the detection of microconcentration of dissolved ammonia was developed using the sol-gel technology. Parameters affecting the sensor performance were evaluated and optimal conditions for the reaction was proposed. Sensor show linear relationship to the concentration of ammonia in a wide range.

Keywords: indicator, sol-gel, absorption, immobilization, ammonia sensor.

1. Introduction.

Ammonia is produced in vast quantities worldwide to produce further fertilizers and as a primary source of nitrogen to prepare a series of chemicals. Main reaction there is known as Haber process and 450 °C and high pressure (100 atm) along with Fe catalyst are used to promote the reaction between hydrogen and nitrogen gas. Ammonia is water soluble weak base and in aqueous solution the following equilibrium is established:

$$NH_{3(aq)} + H_2O_{(l)} \leftrightarrow NH_4^+{}_{(aq)} + OH^-{}_{(aq)}$$
$$pK_b = 4.75$$

And main emission sources of ammonia to aqueous media in environment are decomposition of biological waste, use of fertilizers, agricultural run-off, and fowl-farm where excretion of waste from domestic birds. As gaseous ammonia is decomposed easily by photolytic reaction, dissolved ammonia in environment causes many problems. Thus monitoring of water quality in polluted places, especially in regions close to farms is utmost important. Because ammonia is notorious to be toxic at concentrations above 25 μg/L (1–3).

Numerous methods of ammonia detection of dissolved ammonia have been proposed. Because of availability of LEDs, photodiodes and cheap fluorescent and non-fluorescent dyes, optical sensor for detection of dissolved ammonia have been developing rapidly [3–6]. Many optical sensors for dissolved ammonia detection use polymer membrane as PVC, PVA or ethylcellulose.

In this paper we use tetraethoxysilane matrix and incorporated a pH-sensitive indicator bromocresol purple using the sol-gel route. Using *i*-butylalcohol leads to improved sensor property because of optimal match with the indicator dye. Developed optical ammonia sensors were investigated in different media and there performance was evaluated.

2. Experimental.

2.1. Materials and methods

Tetraethoxysilane (TEOS) was purchased from Haihang Industry Co., Ltd (PRC); ethanol (EtOH), bromocresol purple (BCP), hydrochloric acid (HCl) and nitric acid (HNO_3) were analytical grade and used without any purification. All buffers and solutions prepared using chemical pure grade reactants and doubly distilled water used as solvent.

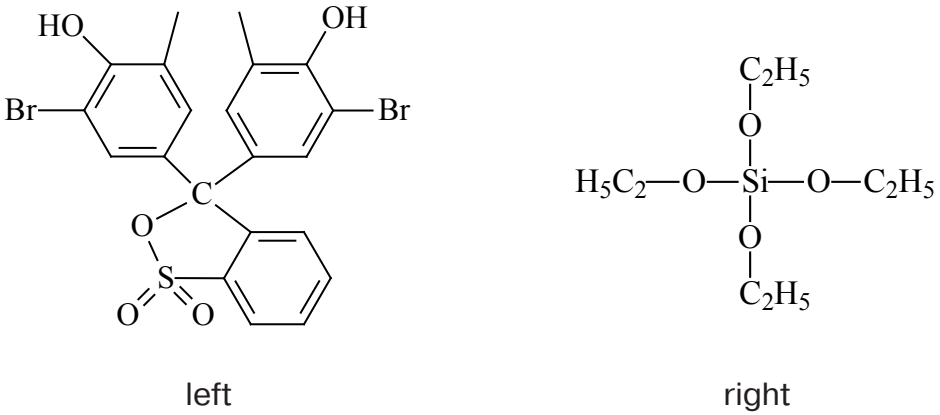

left right

Scheme 1. Structure of BCP (left) and TEOS (right)

2.2. Standard solutions

Ammonia test solutions were prepared using 25% (mass) aqueous concentration of ammonia solution and consequently diluted to reach the desired concentration. Doubly distilled water was used to prepare all solutions throughout the experiment. In order to keep solutions concentration constant, fresh test solutions were used in each experiment.

2.3. Preparation of sol-gel membranes

Sol-gel solutions were prepared mixing 2 ml of TEOS, 3.31 ml of *i*-C_4H_9OH for 30 minutes. 1.3 ml 0,01M HCl aqueous solution was added in order to start hydrolysis and condensation reactions. pH of the final solution was adjusted to 2 since this solution was found to be optimal. Resulting solution was mixed for 4 hours at room temperature. Then 40 μl of 0.1M BCP in C_2H_5OH solution was added and another 30 minutes was mixed. In order to study water to alkoxide ratio *R* several sol cocktails were prepared and the content is given in (Tab. 1).

Table 1.– Content of solutions used in experiment

No.	Alkoxide	Solvent	R ratio	Catalyst
1.	TEOS	*i*-C_4H_9OH	1:1	HCl
2.	TEOS	*i*-C_4H_9OH	1:2	HCl
3.	TEOS	*i*-C_4H_9OH	1:3	HCl
4.	TEOS	*i*-C_4H_9OH	1:4	HCl
5.	TEOS	*i*-C_4H_9OH	1:5	HCl
6.	TEOS	*i*-C_4H_9OH	1:6	HCl

Solution of sol then remained for 24 hours for aging. Microscope slides were taken and cut into 0.6x4 cm pieces. All glasses were activated in the aqueous solution of nitric acid for 1 hour and rinsed with ethanol and copious amount of water before dip coating process. Preparation steps of samples are given in (Fig. 1).

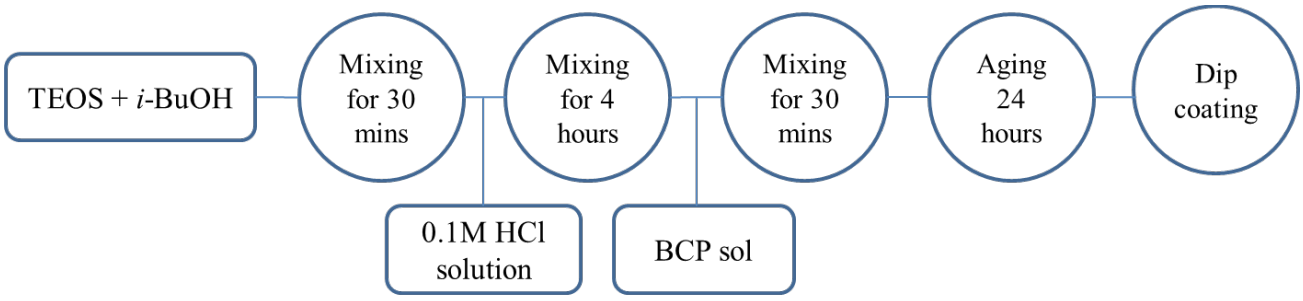

Figure 1. Schematic diagram of sample preparation steps.

2.4. Spectroscopic studies of prepared membranes

UV-vis spectrophotometer EMC-30PC-UV (EMC Labs Germany) was used to record the absorption spectra of the sensors. The surface of the sensor films was investigated using the Optika (Germany). Sensor membranes was rinsed in distilled water and dried before each experiment.

3. Results and discussion.

Measurements were made after one week prior the gelation process completed. All sensor samples were kept in a sealed polymer bag. Sensor layers show no deterioration or any significant change during preservation. In aqueous ammonia solution sensor films converted to violet color immediately. This shows pores of sol-gel film perfectly fulfill to serve as a membrane for the selected indicator dye. Moreover spectrochemical properties of BCP show no change during the immobilization process. This is very crucial, since non-covalent attachment of dye molecule is driving force to maintain photochemical properties of the dopant.

Figure 2 show the absorption spectra of BCP in different aqueous ammonia solutions. BCP shows an intense peak around 590 nm in basic media. Increase in ammonia concentration also increases the intensity of the peak.

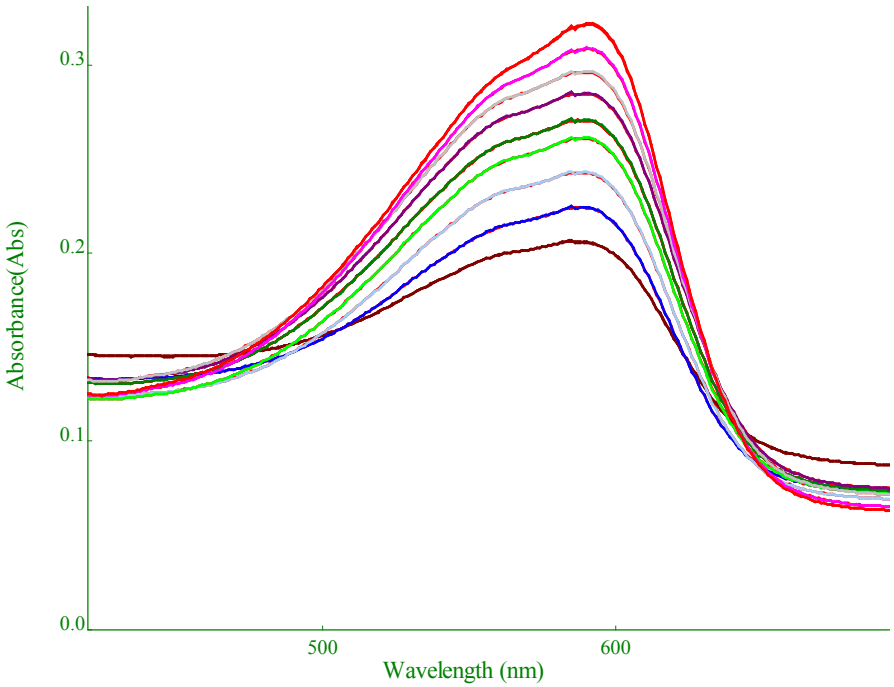

Figure 2. Absorption spectrum of BCP@TEOS sensor in different concentrations of aqueous ammonia (red – 1M, black – 0.2M). Intensity at 588 nm decreases as the concentration of ammonia decreases

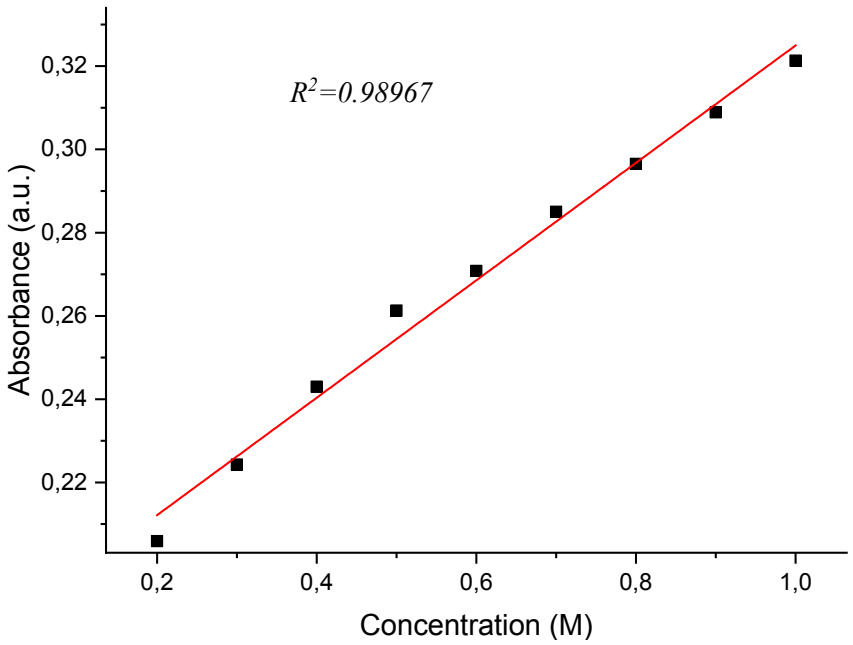

Figure 3. Calibration curve of BCP@TEOS sensors for aqueous ammonia detection

The calibration curve of the sensor is shown in Figure 3. As can be seen from the figure, the absorbance and the concentration shows a good linear relationship in the range of 1M to 0.1M concentration. We also performed experiments with higher ammonia concentrations, but deviation observed in the linear relationship. Possible reason may be related of saturation of the sensor film with $NH_{3(aq)}$ and regeneration of sensor films have little effect on the stable signal reproduction.

Using other solvents as CH_3OH, n-C_3H_7OH, *i*-C_3H_7OH show similar behavior, but the surface shown more cracks and we decided to use i-C_4H_9OH as a solvent. Moreover sensors prepared using *i*-C_4H_9OH show significant improvement in the sensor quality and no practical leaching was observed.

The study also aimed to investigate different parameters to the sensor. For this purpose sensor layers are subjected to hot solutions and other acidic solutions. The sensors show stable response at different temperatures. As the sensing scheme is based on the pH-change, effect of pH was not studied. Acidic media does not interfere to determine dissolved ammonia.

Sensors stored in a sealed polymer bag remained stable for 6 months. However the initial absorbance shown little decrease in intensity.

Conclusions

Optical sensor for the determination of dissolved ammonia is developed. The sensor shows a linear relationship to the concentration of ammonia in a wide range. Effects of different parameters also studied during the experiment. Sensors shown stable response to dissolved ammonia in different conditions.

References:

1. Timmer B., Olthuis W., van der Berg A., Sens. Actuators B107, 2005.– P. 666–677.
2. Porello S., Ferrari G., Lenzi M., Persia E. Aquaculture 219, 2003.– P. 485–494.
3. Waich K., Mayr T., Klimant I. Talanta 77, 2008.– P. 66–72.
4. Lieberzeit P. A., Dickert F. L. Anal. Bioanal. Chem. 387, 2007.– P. 237–247.
5. Malins C., Butler T. M., MacCraith B. D. Thin Solid Films 368, 2000.– P. 105–110.

https://doi.org/10.29013/AJT-19-11.12-29-32

Lobova Elena Gennadievna,
master student, D. Mendeleev
University of Chemical Technology of Russia,
E-mail: promel14@gmail.com
Razheva Tatyana Mikhailovna,
postgraduate student, D. Mendeleev
University of Chemical Technology of Russia
Kurakov Vladimir Vasilievich,
Candidate of Chemical Sciences,
D. Mendeleev University of Chemical Technology of Russia
Kuskov Andrei Nikolaevich,
doctor of Chemical Sciences, D. Mendeleev
University of Chemical Technology of Russia

STUDY OF THE CHARACTERISTICS OF CHITOSAN NANOGELS

Abstract. This work is devoted to the study of the basic physicochemical characteristics of new chitosan nanogels, namely, the determination of the degree of deacetylation, molecular weight, viscosity, particle size, and zeta potential of nanoparticles.

Keywords: chitosan, nanoparticles, gel.

Chitin is one of the most common biopolymers in the world, obtained on an industrial scale. As sources of chitin raw materials, the outer shells of various crustaceans, including crab and shrimp shells, can be used. Chitin deacetylation reaction produces chitosan – a substance that has great potential to be used as a basis for biomedical, pharmaceutical, food and cosmetic products due to its biological compatibility and biodegradability [1].

Chitosan-based materials are used as delivery systems for biologically active and medicinal substances, and it is possible to create various forms of their introduction into the body, such as oral, nasal, parenteral and transdermal dosage forms, as well as biodegradable implants [2].

In addition, it was shown that chitosan has antiviral and antiphase activity; therefore, there are examples of its use in agriculture and food industry. The introduction of chitosan can reduce the growth rate of certain bacteria, infections, and also improves the protective functions of plants [3].

Due to the unique combination of chitosan properties, in recent years there has been growing interest in its use in the field of nanotechnology for the manufacture of a wide range of functional materials for the biomedical industry. For example, the development of liposomes coated for stabilization and protection of chitosan is known, which can be used in tissue engineering, drug delivery, wound healing, etc [4]. However, the niche for the use of chitosan nanoparticles in cosmetics is not yet occupied.

In the present study the main characteristic physicochemical parameters of chitosan were studied to understand the possibility of further application of these gels as the basis of cosmetic and pharmaceutical products.

The object of the study was chitosan produced by Pharm-Region LLC (Moscow), and hydrogels

based on it. To prepare the gel a calculated amount of an aqueous suspension of modified chitosan was added to the beaker, then, constantly stirring, lactic acid was added dropwise, the reaction was stopped when the pH reached 5.2–5.6. The result was a clear gel with slight opalescence.

Chitosan is formed by N-deacetylation of a chitin molecule. The proportion of deacetylated units, defined as the degree of deacetylation (DD), usually rotates from 70 to 90%. This parameter may vary depending on the source of chitin and processing methods. DD was evaluated for chitosan used in the work by using infrared spectroscopy (Nicolet 380 FT-IR), which resulted in 67 ± 1.5 wt.% (Fig. 1).

An equally important parameter is the molecular weight (MW) of polymer. To determine the average-weight MW the viscometric method was used and the MM was 266 ± 4 kDa.

The viscosity of the gels was measured on a Lamy Rheologe RM 200 instrument. The chitosan content's increasing in the gel correlates with the viscosity increasing (Fig. 2). It is also important to note the high thermal stability of gels containing chitosan over 1 wt.%, as their structure remained stable when heated above 100 °C.

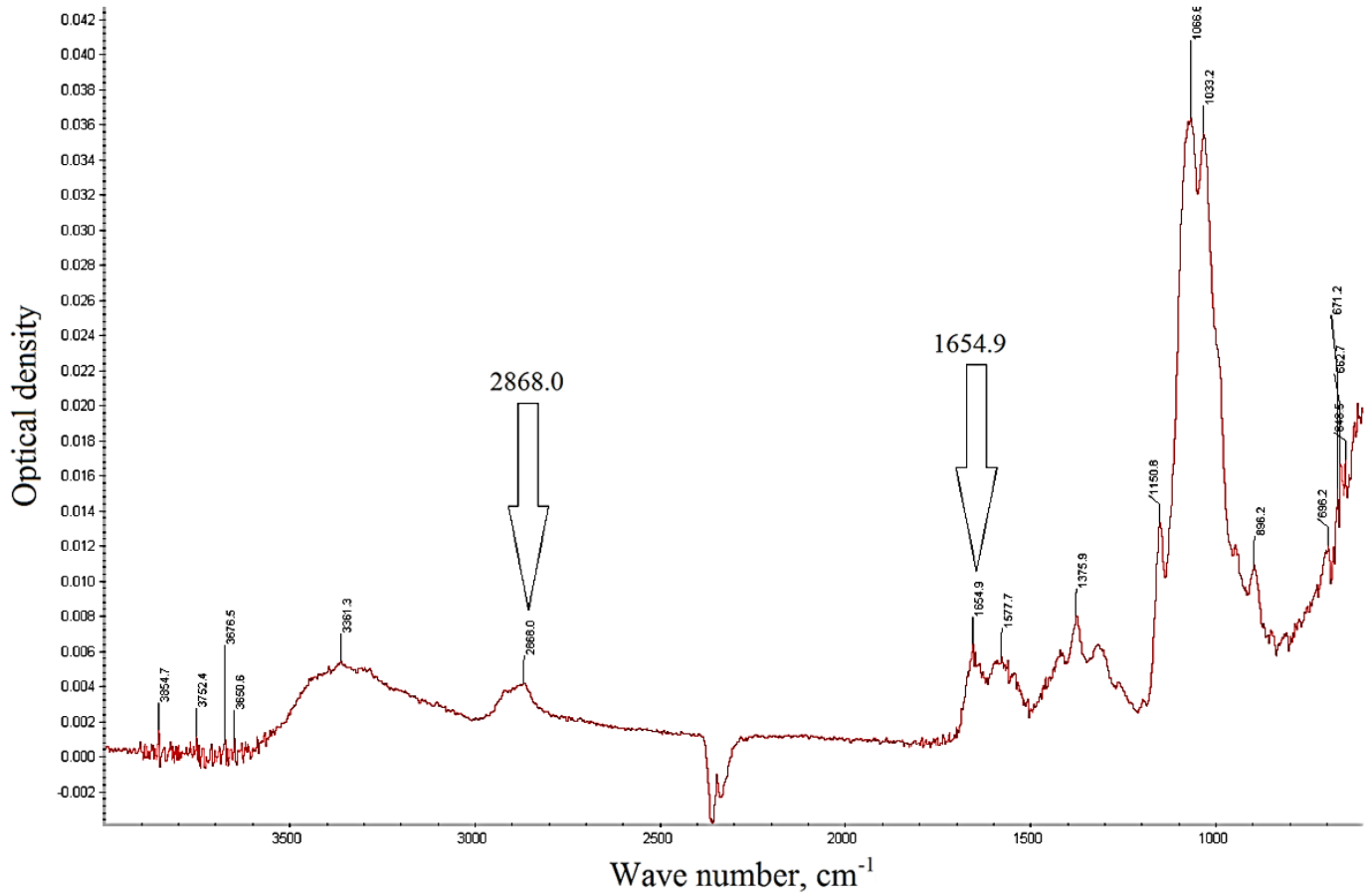

Figure 1. IR-spectrum of chitosan gel

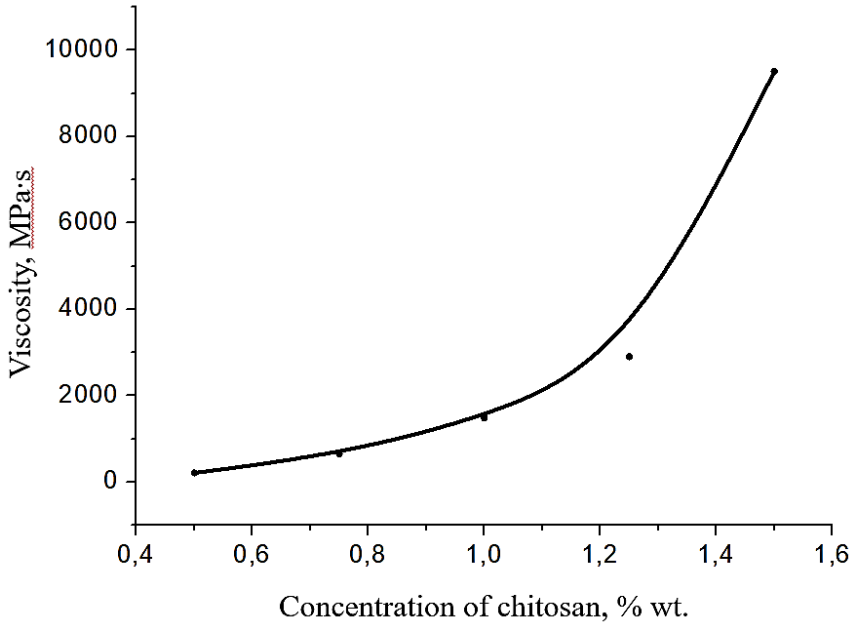

Figure 2. Viscosity curve of chitosan gels

The average diameter and zeta potential of the resulted gels were determined using the Zetasizer Nano ZS-ZEN3600 particle size analyzer at 25 °C. The measured average particle diameter was 70–80 nm (Fig. 3). It is significant to mention that there were no larger aggregates in the system, which means that the structure obtained is quite stable. The particle surface charge is 25 ± 3 mV.

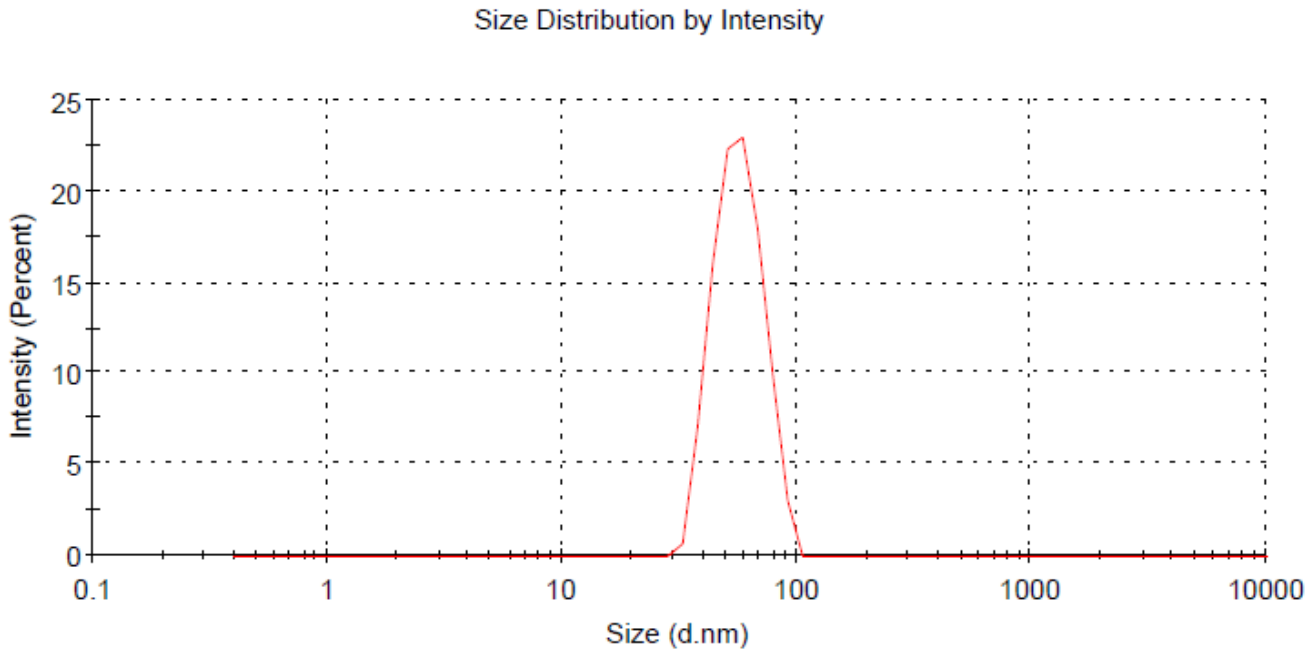

Figure 3. Chitosan gel particle size

Since the purpose of the work is to develop the basis for cosmetics products from chitosan gels, it was necessary to evaluate the effectiveness of various preservatives for the developed gel systems. For this study we selected next preservatives variants: KemNat, KemNatβ and Stabil zero (Akema, Italy); Euxyl 903 (Shulke, Israel), Cosphaderm LA-T (Cosphatec, Germany), Optiphen DLP (Ashland, USA). By the method of microbiological control of perfumery and cosmetic products, it was revealed that the preservative KemNatβ (1%) showed the best effect in the sample of chitosan hydrogel, reducing the number of microorganisms by 93.7% within 7 days compared to the control sample without preservative (Fig. 4).

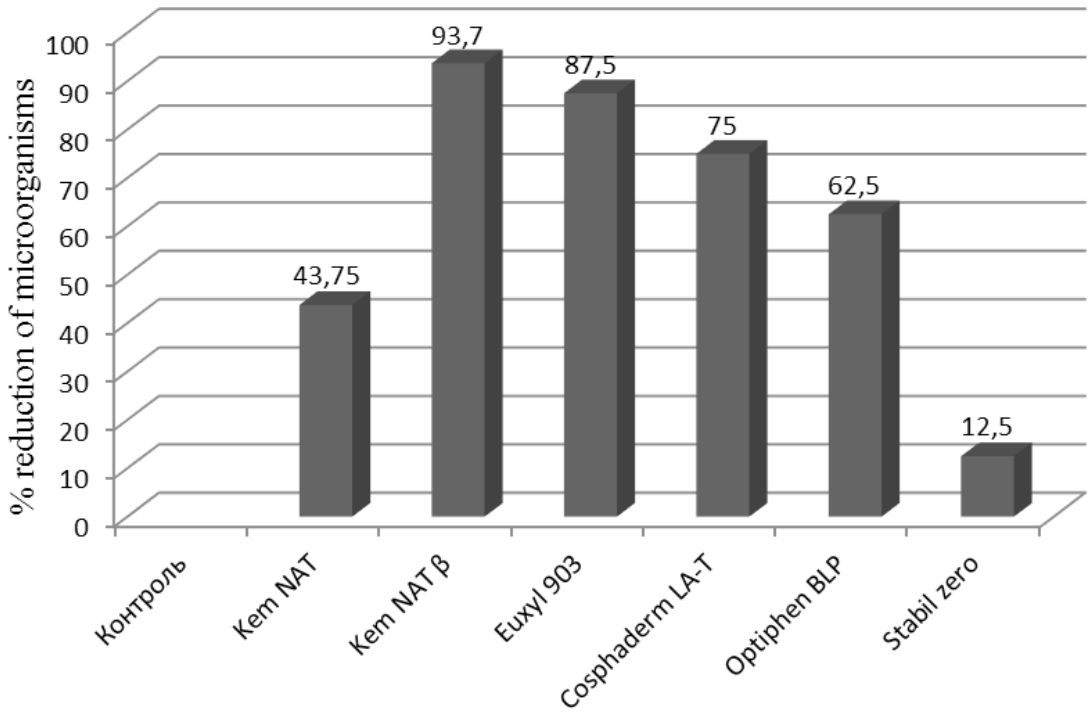

Figure 4. Preservative efficacy in chitosan gel samples.

Thus, today chitosan is widely used in the pharmaceutical and biological fields, while studies on the possibilities of its use in cosmetic products are less common. The results of the studies of the main physicochemical characteristics of the new nanostructured chitosan gels presented in this paper showed good potential for their use, therefore, further development of cosmetic formulations based on the studied gels is planned.

References:

1. Anitha A., Sowmya S., Sudheesh Kumar P. T., Deepthi S., Chennazhi K. P., Ehrlich H., Tsurkan M., Jayakumar R. Chitin and chitosan in selected biomedical applications.– Prog. Polym. Sci., 2014 (39).– P. 1644–1667.
2. Auzely R., Rinaudo M. Controlled chemical modifications of chitosan characterization and investigation of original properties.– Macromol Biosci, 2003 (3).– P. 562–565.
3. Doares S. H., Syrovets T., Weiler E. W., Ryan C. A. Oligogalacturonides and chitosan activate plant defensive genes through the octadecanoid pathway.– Proc.Natl.Acad.Sci. 1995 (92).– P. 4095–8.
4. Ng W. L., Yeong W. Y., Naing W. Y. Polyelectrolyte gelatin-chitosan hydrogeloptimized for 3D bioprinting in skin tissue engineering.– Int. J. Bioprint, 2016(2).– P. 53–62.

https://doi.org/10.29013/AJT-19-11.12-33-37

Mamadoliev Ikromjon Ilkhomidinovich,
Tashkent research institute of Chemical Technology
E-mail: xurshiduz@yandex.ru

STUDY OF THE SORPTION AND TEXTURAL PROPERTIES OF BENTONITE AND KAOLIN

Abstract. The sorption, textural, and physicochemical characteristics of bentonite and kaolin are investigated. To determine the relative surface of the samples, the Brunauer-Emmett-Teller method (BET) was used, and the Barret-Joyner-Helend method (BLC) was used to determine the volume and size of pores. As a result of the research, a relationship was established between the volume of adsorbed gas and the relative pressure and pore radius. It has been established that at P/P_0 = 0–0.05 in the mesopores monomolecular adsorption is observed, at P/P_0 = 0.05 simultaneously mono- and multimolecular adsorption, at P/P_0 = 0.05–0.4 there is a polymolecular adsorption.

Keywords: bentonite, kaolin, colloidality, swelling, adsorbed gas volume, adsorption capacity, meso and micropores.

Introduction

Adsorption methods for industrial hydrocarbon purification are one of the most common methods in the industry. Their use allows a number of valuable compounds to be returned to production in order to reuse. The most important requirements for adsorption materials are: high specific surface area, selective responsiveness and easy regeneration [1–4]. In addition, the adsorbent should be cheap and harmless, with no corrosive properties, should retain its adsorption feature for a long time, and be highly mechanically durable. One of the most common adsorbents is activated carbon and is produced by various brands. In recent years, natural and artificial zeolites have been widely used in the purification of hydrocarbons. One of the most important areas for now is the development of environmentally friendly sorbents, catalysts and catalysts based on local raw materials [5–7].

Experimental

To determine the chemical and physicochemical characteristics, we placed sample granules in 100 g of mass in a 250-cm glass tube and poured 150 cm^3 of distilled water. The flask was stirred for 24 hours on the AVU-6 unit at 120 rpm. After drying, the adsorbent was passed through a sieve with 0.5- and 0.25-mm diameter, and the mechanical and physicochemical properties were studied. Before acid treatment, we grinded the soil samples until to reach particle size 0.08 mm. We added 40 ml H_2SO_4 heated to 10 g of grinded soil and stir in a water bath. After processing, the soil was filtered through a paper filter in the Buchner funnel and washed with distilled water at pH = 5.4–5.7. The soil was then dried with the filter paper in the dryer for 12 hours at 120 °C. Specific surface area and the distribution of pore sizes were found in the automatic adsorbometer ASAB2010 by the low-temperature nitrogen desorption method. Sediment analysis was performed on water and glycerol mixture in different dispersion environments using the Oden method.

X-ray diffraction analysis (Co-Kα-radiation) was performed on the DRON-4 diffractometer with a cobalt X-ray tube. The PDF-2 database of the International Center for Diffraction Data (JCPDS, 1999) was used for the analysis of diffractograms. The porosity of the samples was determined by Quantrome NOVA (USA) analyzer of low-temperature nitrogen

desorption. Each sample was dehydrated for 2 hours at 250 °C under vacuum prior to measurement.

The Brunauer-Emmett-Teller (BET) method was used to determine the relative surface of solid samples. This method is used by the following BET equations:

$$\frac{1}{W\cdot\left(\frac{P_0}{P}-1\right)}=\frac{1}{W_m\cdot C}+\frac{C-1}{W_m\cdot C}\cdot\frac{P_0}{P}.$$

where W–P/P_0 is the adsorbed mass at a relative pressure, W_m – the adsorbed mass on the surface coated a monolayer; S – is a BET constant, which shows the adsorption effect of adsorbents and represents the adsorption energy of the first adsorption layer.

The Barrett-Joyner-Halenda (BJH) method was used to determine the volume and the size distribution of pores. In the calculations, the desorption and adsorption areas of the isotherm with a pressure range of 0.967–0.4 P/P_0 were used.

To determine the shear density, the sorbent weighed 500 g and was kept in the dryer for 600 h at 60 °C. 400 g of the dried sample was weighed and placed in a 500 ml cylinder, measured a volume V_1. We then densified th sorbent by light tapping under the cylinder and t and again measured a volume V_2.

The bulk density of the sorbent was determined by the following formula:

$$\gamma_1=\frac{P}{V_1}.\ \gamma_2=\frac{P}{V_2}.\ [\text{g/cm}^3]$$

where P is the mass of the sorbent; Density of -sorbent and subsequent bulk density, g/cm^3.

Results and discussion

The subject of the study was the Navbakhor bentonite and Pahtachi kaolin.

Table 1.– Chemical content of bentonite in Bavbakhor district

Name	SiO_2	TiO_2	Al_2O_3	Fe_2O_3	MgO	CaO	Na_2O	K_2O	P_2O_5	SO_3
Alkali bentonite soil	57.91	0.35	13.69	5.10	1.84	0.48	1.53	1.75	0.43	0.75
Alkali earth soil	56.23	0.61	13.56	6.50	3.76	0.69	0.98	2.20	0.92	0.49

Prior to acidification of bentonite or kaolin, the sample was heated at 150 °C for 30 min to remove water.

Mass% after acidic acid:

SiO_2–70.17, Al_2O_3–9.49, Fe_2O_3–1.39, MgO-0.64, Na_2O–0.17, K_2O–1.27, CaO–0.20, TiO_2–1.63, MnO–0.01.

Table 2.– Dependence of the activation mode on the physicochemical properties of soil

Porperties of soil	Activation time, seconds								
	0	10	20	40	60	80	100	120	180
Navbakhor bentonite									
Swelling, mg/g	15	18	19.6	22	24	26	27	28	25
Colloid property,%	49	51.6	55	62.2	67.7	70.2	74.7	80	70.9
Water absorption,	2.5	2.46	2.42	2.38	2.36	2.34	2.32	2.3	2.45
Pakhtachi kaolin									
Swelling, mg/g	25	28	29,6	30	33	36	38	42	44
Colloid property,%	89	90	92	94	96	96	99	100	100
Water absorption	10	12	14	16	18	20	22	28	30

Table 3.– Physical characteristics of natural soil

	Pakhtachi kaolin	Navbakhor bentonite
1	*2*	*3*
Specific surface are, m^2/g	250–300	125–200

1	*2*	*3*
Bulk density, kg/m^2	600–700	570–650
Pore volume, cm^3/g	0.028–0.041	0.048
Pore size, nm	2.6–2.8	3.4–4.3

In the equilibrium mode, the adsorption test allows to determine the maximum adsorption rate and to calculate the thermodynamic parameters of adsorption at low temperature fluctuations.

Adjusting the adsorption equation by the experimental design of adsorption isotherms is accepted. The expression of adsorption by Langmuir and Freundlich models is widely used in the literature:

$$\frac{\alpha}{\alpha_\infty}=\frac{K_L\cdot C_0}{1+K_L\cdot C_0}.\quad \alpha=K_F\cdot C^{on\ldots}\quad \frac{\alpha}{\alpha_\infty}=\frac{K_L\cdot C^{on}}{1+K_L\cdot C^{on}}.$$

$$\frac{C/C^0}{\alpha 1-\frac{C}{C^0}}=\frac{1}{\alpha_\infty\cdot C}+\frac{k-1}{\alpha_\infty kC^0}$$

where $k=e^{\frac{Q-\lambda}{RT}}$ thus $Q-\lambda$ – adsorption heat

$$\frac{\alpha}{\alpha_\infty}=\frac{K_R\cdot C^0}{1+\alpha\cdot C^{0\beta}}.$$

α,β – Redlich-Peterson equation parameters

There is a relationship between the adsorption equation and the change in adsorption enthalpy and entropy:

$$K_{\alpha ds}=e^{\frac{\Delta S_{\alpha ds}}{R}}\cdot e^{\frac{\Delta H_{\alpha ds}}{RT}}$$

The rate of adsorption process can be expressed in time units by changing the amount of adsorbed substance in the mass of the adsorbent as follows:

$$r_{\alpha ds}=\frac{d\alpha}{d\tau}\ [(\text{mg/g})/\text{s}]$$

Thus, the mass of adsorbed substance in $\alpha-1$ g of adsorbent, – the time.

The following expression is important for the dynamic system in an open system, such as the flow adsorber:

$$V=\frac{W\cdot dC}{S\cdot dL}=\frac{W\cdot dC}{dV_{\alpha ds}}$$

where V – is the rate of the adsorption process, W – the volume rate of the current; C – reactor cross-section surface, l – adsorbent layer height; V_{ads} – the volume of adsorbent.

Studies have shown that the adsorption process is subject to a 2-order reaction equation:

$$\frac{d\alpha}{d\tau}=\frac{k_2\cdot\left(\alpha_\infty-\alpha_\tau\right)^2}{1+k_2\cdot\left(\alpha_\infty-\alpha_\tau\right)}\approx k_2\cdot\left(\alpha_\infty-\alpha_\tau\right)^2$$

Or its integrated form is as follows:

$$\frac{\tau}{\alpha_\infty}=\frac{1}{k_2\cdot\alpha_\infty^2}+\frac{\tau}{\alpha_\tau}$$

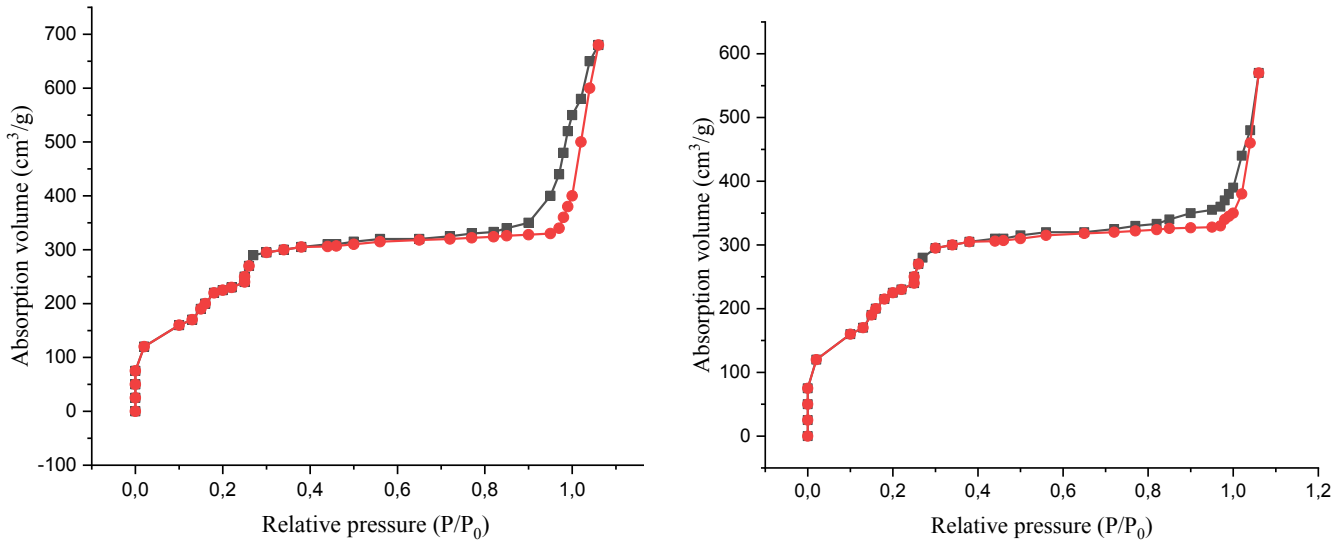

Figure 1. Adsorption-desorption isotherms of nitrogen in mesopores of synthesized sorbents

Diffusion model for the adsorption process:

$$\alpha_\tau = k_{diff} \cdot \tau^{\frac{1}{2}} + S$$

k_{diff} – diffusion constant of the adsorption rate, S-constant number.

Dynamic capacity of the adsorbent is found using the formula:

$$\alpha_d = \frac{P_m \cdot V \cdot [S]}{m_{\alpha ds}}$$

Comparison of surface and microwave size was calculated by BET method for mesoporous sorbents and Dubinin method for mesoporous sorbents. To confirm the structure of the sorbents, we present the nitrogen adsorption desorption curves for mesoporous sorbents(Figure 1).

As shown in Figure 1, the adsorption-desorption isotherms presented are typical of type IV isotherms. We consider the distribution of pore size for the synthesized porous sorbents (calculated by the BJH method).

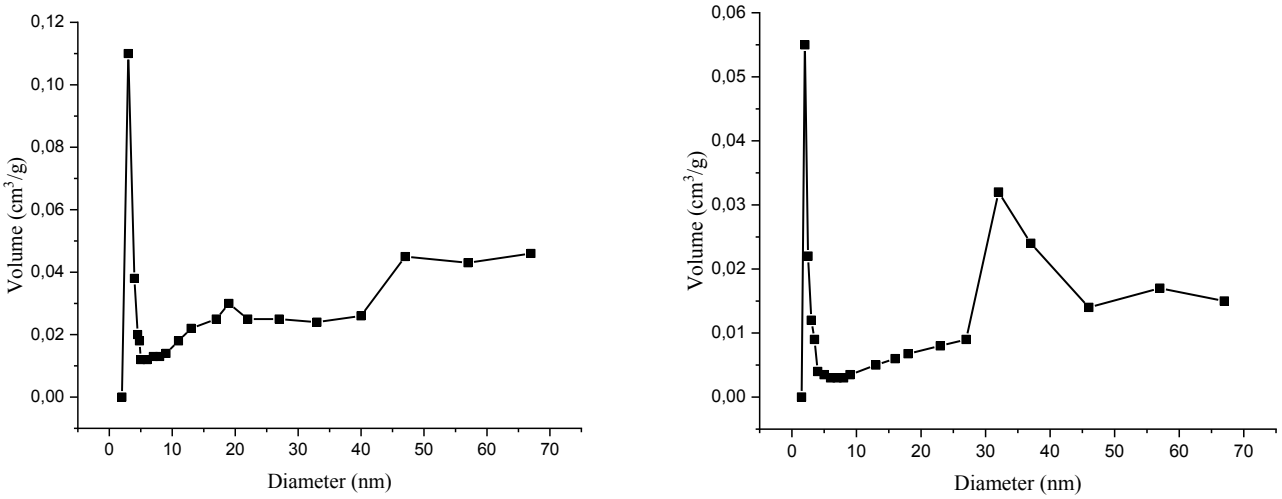

Figure 2. Pore volume distribution depending on diameters of mesoporous sorbents

As Figure 2 shows, the synthesized porous sorbents consist mainly of pore volume around 2 nm.

Microporous sorbents provide characteristic isotherms of nitrogen adsorption.

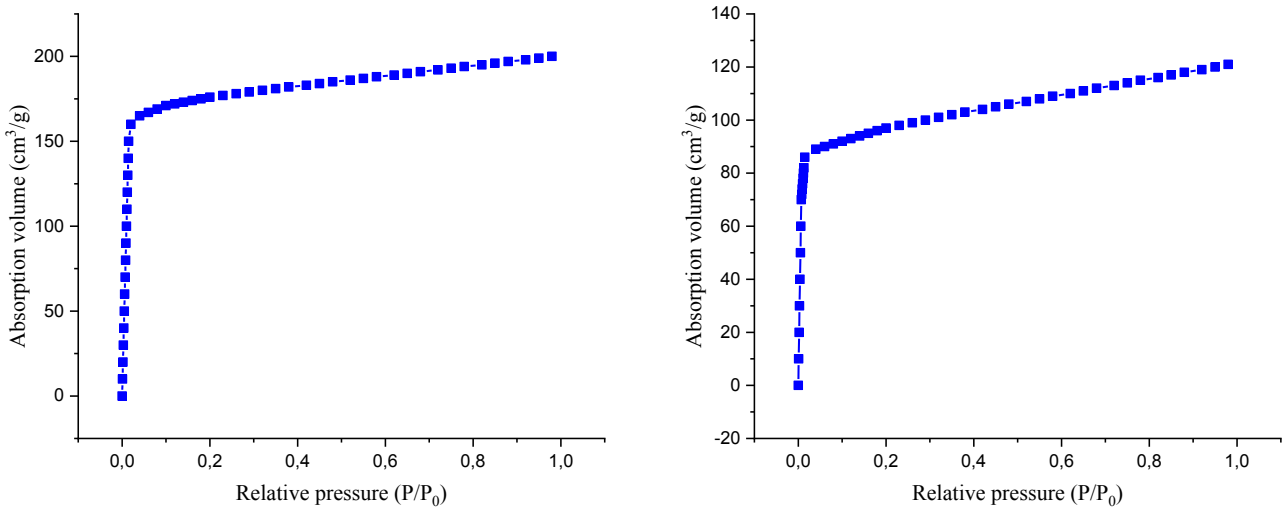

Figure 3. Nitrogen adsorption-dsorption isotherms in micropores of microporous sorbents

As can be seen from Figure 3, the isotherms present are of the first type of isotherms (horizontal planes present).

Conclusions

1) The sorption, texture and physicochemical characteristics of bentonite and kaolin were studied.

2) The Brunauer-Emmett-Teller (BET) method was used to determine the specific surface areasof the samples, and the Barrett-Joyner-Halenda (BJH) method to determine the pore volume and size distribution.

3) The study investigated the relationship between adsorption volume and relative pressure and pore radius.

4) Monomolecular adsorption at the interval P/P_0 = 0–0.05, mono- and polymolecular adsorption at the interval P/P_0 = 0.05, and P/P_0 = 0.05–0.4 polymer molecular adsorption processes have been proven.

References:

1. Shukurov B. Sh., Rakhmatov Sh. B., Fayzullayev N. I. High silicon zeolite preparation from kaolin // Scientific journal of SamSU, 2018. 5(109),– P. 106–111.
2. Ayari F., Srasra E., Trabelsi-Ayadi M. Characterization of bentonitic clays and their use as adsorbent // Desalination. 2005.– Vol. 185.– No. 1–3.– P. 391–397.
3. Vezentsev A. I., Volovicheva N. A. The material composition and sorption characteristics of montmorillonite containing clay // Sorption and chromatographic processes. 2007.– Vol. 7.– No. 4.– P. 639–643.
4. Sadykov T. F., Konkova T. V., Alekhina M. B. Montmorillonite with a laminated structure for the fenton process // Advances in Chemistry and Chemical Technology. 2012.– Vol. 26.– No. 8 (137).– P. 50–54.
5. Mostalygina L. V., Chernova E. A., Bukhtoyarov O. I. Acid activation of bentonite clay // Bulletin of the South Ural State University. Series "Chemistry". 2012.– No. 24. P. 57–61.
6. Volkov V. A. Colloid chemistry. Surface phenomena and disperse systems // – M.: Lan, 2015.– 256 p.
7. Kosarev A. V. Modeling the kinetics of adsorption of natural structures on a polymer matrix / A. V. Kosarev, N. V. Vedeneeva, E. I. Tikhomirova // Modern bioengineering and nuclear-physical technologies in medicine: Sat. Mater. vseros. young scientific conf. / holes ed. V. N. Lyasnikov.– M.: Prondo, 2014.– P. 305–308.

https://doi.org/10.29013/AJT-19-11.12-38-40

Mamedov Elnur Shamhal,
leading researcher,
Veliyeva Dilara Safar,
leading researcher,
E-mail: chem@science.az
Kulibekova Tamilla Nasraddin,
leading researcher,
Rushinaz Irada Rahim,
researcher,
Aliyeva Fidan Maharram,
researcher, Azerbaijan National Academy of Sciences,
Institute of Catalysis and Inogranic Chemistry
named after acad. M. Nagiyev, Baku, Azerbaijan

RECYCLING OF THE OVERDUE PRESCRIPTIONS (RD) FOR DEGASSING OF TOXIC SUBSTANCES

Abstract. The constant source of environmental pollution besides the other harmful substances is presence of different chemically poisonous toxic substances, as well as special chemical solutions and prescriptions. The latter are removed from the surface of contaminated objects of military technique, weapons and local place by the method of degassing. In this article we present the data on degassing the educational prescriptions RD-2 and RD-A where their physical-chemical indexes have been determined.

Keywords: utilization, recycling, educational prescriptions RD-2 and RD-A, toxic substances.

Introduction

In contemporary life lots of military bases stand in front of the fact about the presence of different chemically harmful poisonous toxic substances, special chemical solutions and prescriptions used in the process of degassing contaminated area, that became the thread for environment because they have been kept too long. That's why at presents time there is an acute question about the utilization of all overdue chemically poisonous substances.

For example, the poisonous substances (PS) are removed from the surface, of contaminated objects of military technique and arms, remedies for individual protection of skin and local place [1–3]. Degassing reagents in contact with the poisonous substances convert them into non-toxic compounds. We differ 2 types of degassing: the first happening naturally at the expence of evaporation and absorbing the poisonous substances, and the second by the artificial way – by means of processing separate sections of the surface, where people are touch. When an accident takes place at the industrial objects or while using the poisonous substances there have been created contaminated zones.

We differ mechanical, physical and physical-chemical degassing of the surface. During mechanical and physical-chemical degassing the poisonous substances are removed from the surface by weathering, by washing with water, but however the poisonous substances themselves don't destroy. While

using the chemical degassing the contaminated by toxic substance surface starts the reaction with degassing prescription with formation of little poisonous and non-poisonous products. In that cases we use the water solutions of alkali, hypochlorites and different chloramines [4], however at temperatures due 0 °C, the hypochlorites become effective less. Besides the substances of oxidative-chloric action at the same time we also use alkaline degassing reagents (caustic alkali, salts, ammonia). The main components coming into the composition of prescriptions are alcoxides of alkaline metals, surfactants proton and aproton solvents, which influence their aggressive action upon varnish-dyeing coats and rubber- technical wares, it also comes to reduce of resistence in electrowires isolation. Water also concerns to the number of degassing substances, which destroys the poisoning substances while boiling, therefore it is used for degassing the clothes and some other remedies of individual defence [5–8].

For degassing the arms, military technique, the open parts of human body, equipment and uniform they usually use poly-degassing prescriptions RD-2 and RD-A. Our researches are devoted to their utilization.

The degassing prescription RD-2 – is a mobile liquid from light-yellow to the brown color, which is aimed for degassing the arms and military technique, remedies of individual defence of the skin and local place, contaminated with VX, "zoman" and "iprit". For an effective degassing with prescription RD-2, the poisoned surfaces of the objects should de dry. Prescription RD-2 has got a wide temperature interval for the usage from +40 °C up to –60 °C, with the temperature of a flash +31 °C. It has been the main prescription for winter conditions.

Some physical-chemical indexes and the composition of RD-2 (%) is given below:

Chlorbenzol-48, Kerosene-37, Isobutyl alcohol-8, Ethylcellozolve, Oxyphos-1.

The standard of expenditure of prescription while poisoning with is 0.4 l/m^2 mustard gas, and for degassing the local place – 1.5–2 l/m^2.

Prescription RD-2 is received by the troops in ready-made type in steel barrels and it may be used in winter conditions. It's flammable. Water drops entering or long-term contact with the atmosphere lead to reduce of degassing ability of prescription. In hermetically closed package the abilities of RD-2 are kept within 5 years, but in case of dis-hermetics they are lost in a week.

As far as after a long-term keeping RD-2 comes unlit state, it is subjected to utilization. Often use on parallel processes: both utilization and liquidation. The utilization leads to further usage of final products with the new consumer qualities.

Degassing prescription of RD-A is intended for a partial degassing of rifle arms, the objects of armoured weapons and technique at temperature from +40 °C up to –37 °C with a standard expenditure 0,4 l/m^2. The prescription is delivered and kept in the steel hermetically closed barrels.

Composition of RD-A: benzene B-70, n-butyl alcohol, ethylenediamine, ethylcellozovle, natrium hydroxide.

Experimental part

As far as the compounds coming into the composition of degassing substances prescriptions RD-2 and RD-A are well-known, the aim of our research is elaboration of the methods of their extraction and their second usage in the industry (recycling).

For utilization there have been made their fractionated distillation at the atmosphere pressure and in vacuum (10 mm of mercury column) in the interval of temperatures from 88 to 250 °C, selecting each fraction separately. Physical-chemical constants have been determined.

Table 1.

Components	n_D^{20}	d_4^{20}	t_{boil} °C
RD-2			
chlorbenzol	1.5248	1.1066	132
kerosene			150–250
kalium isobulat in mixture with isobutanol	1.3977	0.8027	108
ethylcellozovle			135.6
oxyphos			
RD-A			
benzene B-70			88
n-bityl alcohol	1.3993		117.7
ethylenediamine	1.4508	0.8977	116.5
ethylcellozovle			135.6

Conclusion

The carried out marketing researches showed that the extracted substances in the process of recycling the degassing prescriptions could find the wide usage in the people's economy. For example, an oxyphos in used in leather, fur industry as a filler, moisten, defatted and washing means with antiseptic effect, as a dispersant of magnet tapes while making a magnet varnish, as an inhibitor of asphalt-resinous and paraffin sediments at the oil transportation through the pipelines. Ethylcellozovle is used as an antifreeze in aircraft fuel with the aim to prevent the freezing of water containing in it. Ethylenediamine is used in production of dyers, emulgators, stabilizators and fungicides. Kerosine has a wide spectrum of usage. It is used both as component of fuel and as a fuel while burning the porcelain and glass wares, and etc.

References:

1. Karpov V. R., Kazimirov O. V., Kapkanets K. S. Scientific-technical analysis of the main directions while creation the new specimens of technical remedies and prescriptions of a special treatment. / auth. V. P. Karpov, O. V. Kazimirov, K. S. Karpanets / Vestnik voisk ROC of defence, 2017.– Vol. 1.– No. 1.– P. 42–52.
2. Bogatiryov V. V. Main problems of perfectioning in russian means of individual and collective protection. Vestnik voisk ROC of defence, 2017.– Vol. 1.– No. 2.– P. 28–39.
3. Alexandrov V. N., Yemelyanov V. I. Poisonous substances. School appliance. Under editorship of Doctor in chemistry, prof. Sokolsky G. A.– second edition, remade and completed – M. Voenizdat, 1990.– 272 p.
4. Chemistry of poisonous substances. 1973.– Vol. 2.– P. 271, 309, 461.
5. Jane's Defence Equipment Library /Jane's NBC Protection Equipment. 2002–2003. 1 electron disk (CD-ROM).
6. Remedies and methods of desactivation, degassing and disinfection. Sanitary treatment of people.– M. 1969.
7. Defence of the objects of people's economy from the weapons of mass destruction. Reference-book / Demidenko G. P., Kuzmenko E. P., Orlov P. P. and oth.– Kiev, 1989.
8. Chemistry of poisonous substances. Franke Z, Varnke V.– Vol. 1–2.– M. 1973.

https://doi.org/10.29013/AJT-19-11.12-38-44

Ismatova Ra'no Axadovna,
Norov Ilg'or Ilxomovich,
Amonov Muxtor Raxmatovich,
Ibragimova Feruza Baxriddinovna,
Bukhara State University
E-mail: sshav85@inbox.ru

SIZING POLYMER COMPOSITIONS ON THE BASE OF STARCH AND POLYVINYL ALCOHOL

Abstract. The article investigates the physicochemical properties of yarn depending on the concentration of starch and polyvinyl alcohol (PVA). It was revealed that the use of the developed polymer composition in the process of sizing cotton yarn made it possible to increase its strength, decrease the ultimate elongation and as the most important indicator contributes to the reduction of yarn breakage.

Keywords: Yarn, starch, PVA, properties, strength, composition, polymer, dressing (sizing solution), concentration, ultimate elongation.

Improving the quality and competitiveness of products is one of the key tasks in the textile industry, resolved by creating effective waste-free technologies that can significantly reduce or completely eliminate the use of expensive imported chemical materials.

Despite significant advances in the field of refinement of cotton fiber, successes in this area are far from exhausted. It remains a very urgent task to develop effective polymeric materials suitable for sizing yarn. Due to the availability of the raw material base, the specificity of the properties of polymeric materials makes it possible to purposefully use yarn in the sizing process, while significantly saving scarce expensive components and ensuring the rhythmic production of textile enterprises [1–4].

The main indicator that determines the quality of sizing in production is the thread breakage during weaving process. However, this indicator can only be determined under the conditions of a particular production, since the breakage is determined by the total influence of a number of factors, including factors not related to the quality of the dressing (yarn quality, humidity in the weaving department, operating mode of the sizing machine, maintaining time of sized yarn before weaving, etc.). There are a number of indicators by which the suitability of the dressing can be determined without carrying out the sizing process. Such important indicators include viscosity, the degree of uncoupling of starch grains, the content of the water-soluble fraction and surface tension.

The main purpose of these studies is to identify the general trend of the influence of various factors on the properties of the dressing and the quality of the sized yarn according to the developed sizing polymer composition.

On this basis, the initial study was aimed at selecting the concentrations of starch, PVA in the composition.

The experiment results for the change in the physical and mechanical properties of the sized cotton yarn with starch and PVA are presented in (Table 1).

As can be seen from Table 1, the magnitude of bursting strength, bursting elongation and pick-

upconsiderably depend on the composition of the dressing. The use of the developed polymer composition on the basis of starch and PVA during sizing of cotton yarn allowed to increase its strength, reduce bursting elongation, and this, in turn, helped to diminish the yarn breakage.

Table 1.– Changes in the physical and mechanical properties of yarn while taking in PVA into dressing

Sizing composition,%		Ratio of starch and PVA in dressing,%	Breaking load P, cH	Breaking elongation E,%	Pick-up K,%
Starch	PVA from the weight of starch				
5	–	100:0	256	10.7	3.7
	1.0	97.5:2.5	264	9.1	4.6
	2.0	95.0:5.0	314	6.4	5.1
	3.0	93.0:7.0	321	5.2	6.8
6	–	100:0	265	10.4	3.6
	1.0	97.5:2.5	286	9.0	5.0
	3.0	95.0:5.0	332	5.7	5.2
	3.0	93.0:7.0	354	4.3	5.4
7	–	100:0	282	9.7	3.5
	1.0	97.5:2.5	310	8.1	5.6
	3.0	95.0:5.0	336	5.2	5.8
	3.0	93.0:7.0	361	4.1	5.9

Moreover, we can observe a significant change in the structural and mechanical properties of the system with an increase in the concentration of PVA from 1.0 to 3.0% in starch paste.

As can be seen from Table 1, not only the starch content, but also PVA has a significant effect on the breaking characteristics of the sized yarn. For instance, if the breaking load of cotton yarn is with 5% starch content, 1.0% PVA is 264 sN, with the same starch content and increase of PVA content to 3.0%, the breaking load will increase to 327 sN, i.e., it will upsurge by 23%.

It is known that under the conditions of complex formation of starch and PVA, significant changes occur in the rheological properties of the system.

It will be possible to significantly modify the physical and mechanical properties of starch dressing by adding PVA in it.

The advantage of PVA compositions as a sizing preparation lies in its high adhesive ability.

The strength properties of yarn sized with the proposed compounds have shown that the strength properties of yarn sized with a 5–7% starch dressing differ significantly from those without PVA (Table 2). In addition, the use of a water-soluble PVA polymer as a part of starch dressing contributes to the maximum decrease in the surface tension of the system and the improvement of the physical and mechanical characteristics of the yarn. Furthermore, in order to let dressing remain on the surface of the fiber in the form of an adhesive film, it must have sufficient viscosity and meet numerous production requirements.

Based on the scientific data and theoretical and experimental research, highly effective dressing polymer compositions consisting of starch and PVA have been developed for various types of yarn (18.5; 20 and 29.4).

Table 2.– Physical and mechanical characteristics of sized and unsized cotton yarn

Dressing		Breaking load P, sN	Breaking elongation (mm)
Unsized		220 ± 5.5	98 ± 1.0
Starch%	PVA,,% of dry weight of starch		
4	–	256	93
5	–	265	87
6	–	282	82
4	1.0	264	78
	2.0	314	72
	3.0	321	66
5	1.0	286	75
	2.0	332	69
	3.0	254	61
6	1.0	310	72
	2.0	335	64
	3.0	361	56

The properties of dressing and the sized cotton yarn are presented in Table 3.

From Table 3 it is seen that the presence of PVA in the dressing composition based on starch, it has a positive effect on the process of gelatinization of starch and helps to increase the breaking strength of the system. For example, at a yarn density of 29.4, the breaking load of the sized polymer compositions is 328.3 sN versus 291.7 sN of sized corn starch.

Table 3.– Properties of dressing made of polymer materials and sized yarn of various types

Parameters	Sizing polymer compositions			Dressing on the basis of starch		
	Yarn density, textile					
	18,5	20	29,4	18,5	20	29,4
Dressing viscosity	2.7	4.4	7.1	1.6	4.2	6.1
Concentration of adhesive material,%	1.5	3.0	4.2	1.6	4.0	4.4
Real pick-up,%	2.1	3.6	4.1	1.8	2.5	3.8
Breakage	0.27	0.29	0.32	0.32	0.41	0.52
Degree of dressing wear,%	96.3	87.2	81.7	78.3	66.4	63.2
Breaking strength, sN	314.5	326.7	328.3	266.7	284.6	291.7
Breaking elongation,%	5.6	4.8	4.4	8.1	7.5	6.8
Breaking yarn length, km	12.7	15.3	16.7	15.1	17.2	18.1
Linear deviation density,%	7.4	7.9	8.6	8.1	8.9	9.5
Deviation of breaking strength,%	9.6	13.4	14.7	12.6	14.0	14.2
Abrasion resistance, sN	1910	2570	3170	2540	3010	3070

In the (Table 3) it is shown that sizing polymer compositions significantly increase the efficiency of a number of technological processes, in particular, sizing. At the same time, it was revealed that the breaking elongation of the sized yarn is inversely proportional to the amount of PVA. The optimal PVA ratio was found, providing breaking strength and elongation corresponding to the production requirements. It has been established that the introduction of low concentrations, up to 5% and PVA up to 3.0% from the weight of starch into starch solutions favorably improve the adhesion of the system to cotton fibers. The degree of dressingwear reaches up to 96.3%. In addition, the use of polymer compositions helps to increase labor productivity by improving a number of technological characteristics, in particular, reducing the thread breakage.

Thus, the study of the dependence of the physicochemical and mechanical properties of sized substrates on the chemical nature and concentration of the dressing components showed that starch and PVA compositions satisfy the requirements for adhesive and film-forming dressing components.

References:

1. Amonov M. R., Khafizov A. R., Davirov Sh.N., Yariev O. M. Влияние состава шлихты на свойства о шлихтованной пряжи. Узбек. Chemical journal. 2002.– No. 5.– P. 64–67.
2. Amonov M. R., Khafizov A. R., Davirov Sh.N., Yariev O. M., Ikhtiyarova G. A. Исследование влияния композиций для шлихтования хлопчатобумажной пряжи на ее качество. Композицион материаллар журнали.– Tashkent, 2002 йил.– № 2.– P. 35–36.
3. Amonov M. R., Khafizov A. R., Davirov Sh.N., Yariev O. M. O. M. Изучение адгезионных свойств полимерных шлихтующих композиций. Журн. ДАНРУз. 2002.– № 5.– P. 27–30.
4. Amonov M. R., Khafizov A. R., Yariev O. M., Ikhtiyarova G. A. Физико-химические основы разработки состава шлихтующих компонентов. Журн. Пластические массы.– М., 2003.– № 6.– P. 32–34.

https://doi.org/10.29013/AJT-19-11.12-45-47

Mazhidov Abdunabi Amonovich,
Mardonova Saodat Muxammadjonovna,
Muratova Gulsara Saidovna,
Bukhara State University
E-mail: sshav85@mail.ru

PRINTING AND TECHNICAL PROPERTIES OF COTTON FABRICS PRINTED BY THICKNING POLYMER COMPOSITIONS

Abstract. The article reveals thecolourstability of printed fabrics of modified and native starch. It also determines that the printing and technical properties, in particular, the degree of fixation of the dye and the intensity of the color, mostly depend on the nature of the thickener. Moreover, it has been established that the use of a new thickening composition for cloth printing leads to an improvement in the quality of printed fabrics.

Keywords: Colour stability, fabric, modification, dye, fixation, properties, thickener, quality.

Printing inks are highly viscous structured systems, and thickening is one of their main components [3]. It prevents the occurrence of undesirable reactions in the ink and counteracts the capillary forces of the substrate, ensuring the sharpness of the printed pattern [1–3].

The choice of products for thickening printing inks is one of the most important problems in the field of printing textile materials.

To achieve the best results, thickeners imparting a high viscosity to the paste paint should be used, as this will make it easier to subsequently wash the thickener from the fabric, it should also have such a color and chemical properties that would not preclude obtaining a pure color and color development [4].

Most natural thickeners used in the textile industry are polysaccharides. In terms of bulk of use, more than 90% of the natural thickeners are various starches and products of their modification [5].

The use of thickeners based on sodium alginate is more attractive, but their high cost due to the limited production of raw materials, inhibits their widespread implementation [7–8].

Today various methods for the modification and improvement of the printing and technical properties of starch thickenershave been proposed. New technological methods of chemical modification have been developed, and preparations have been created for the modification of starch directly in the conditions of textile enterprises. The main idea of the developed technological methods is the introduction of functional polymer compounds with carboxymethyl cellulose of natureinto hot starch paste, capable of adsorbing colloidal starch particles, preventing their aggregation, due to which the necessary rheological properties of the obtained product are achieved. To modify the starch in this way, the preparationcalled *Printactive*was developed, which imparts a negative electrokinetic potential to colloidal starch particles, and therefore, to a lesser extent than unmodified thickener, forms covalent bonds with active dyes.

Chemically modified starch-based thickeners were tested in the printing of cotton fabrics with active dyes, the results of which are presented in Table 1.

Data presented in Table 1 show the replacement of common thickeners with chemically modified starch leads to a significant increase in the degree of colour fixation and the color intensity; reduce the stiffness of the printed fabric and improvement of the strength indicators of patterned colours of textile.

Table 1.– The impact of the nature of the thickener and the methods of its modification on the coloristic properties of cotton fabrics, printed by ostazine bright red active dyes

Name of the thickener	Method of modification	Thickener concentration gr/kg	Colour intensity, K/S	Colour stability, Mark			Fixation degree of active dyes,%
				Washability	Perspiration	Dryness	
Starch	Unmodified	80	14,2	4/4/4	4/4/4	5	72.6
Starch composition	Bare	50	23.8	5/5/5	5/4/5	5	87.4

Table 2.– Printing and technological properties of alginate, modified and native starch in cloth printing

Dye	Fixation degree of active dye.%			Colour intensity. K/S		
	Alginate	Modified starch	Native starch	Alginate	Modifies starch	Native starch
Vatb right green	87.4	85.3	72.6	14.26	12.87	10.28
Procion bright orange	85.3	84.6	71.2	12.16	11.84	7.65
Cibacroneb right red	91.6	89.4	81.2	16.43	15.75	12.16
Remazolb right red	93.2	91.6	82.3	14.74	14.22	9.65

One of the main indicators of printed fabrics is the colour stability, i.e. their washing out capacity. In this regard, further studies are aimed at determining the amount of dye in the washing trough, itsfixation on the fiber and non-fixation on the fabric. The samples underwent thermo fixation and steaming processes after printing, and the capacity of washabilityof the dye was determined depending on the temperature, duration of washing, and type of dye. The research results are presented in Table 3.

Table 3.– Dependence of the degree of fixation of dyes and their washability out capacity on the type of thickener

Thickeners	Temperature of washing trough, °C	Amount of the dye,%					
		Active bright purple 4K			Active bright red 5SX		
		In washing trough	Fixed on the fabric	Non-fixed on the fiber and remained on the fabric	In washing trough	Fixed on the fabric	Non-fixed on the fiber and remained on the fabric
Maize starch	80	18.4	50.2	31.4	19.5	53.7	26.3
Starch oxidizedwith-manganoussulphate	80	11.9	71.6	17.5	11.3	73.0	15.7
Starch modified with carboxymethyl cellulose and sericin	80	8.2	72.3	19.5	9.3	74.3	16.4

As can be seen from the data in (Table 3), the fixation of the dye with fiber thickeners made of modified starches which are obtained by oxidation using manganoussulphate and modified car-

boxymethyl cellulose and sericin is approximately the same and it is 25% higher than ordinary starch thickening. When comparing printed formulations with ordinary starch and modified one, in the third case, not only the degree of fixation is greater, but also the amount of nonfixed dye remaining on the fabric is reduced, which helps increase the color stability to wet treatments.

Thus, as a result of evaluating the effectiveness of the developed thickener composition, it was found that the use of new thickening compositions improves the quality of cloth printing, increases the environmental friendly textile materials and reduces the material and resource intensity of cloth printing processes by 1.5 times.

Conclusion

1. New water-soluble polymer compositions have been pioneered as a thickener for printing cotton fabrics on the basis of starch, carboxymethyl cellulose and sericin and their basic physical and mechanical properties have been thoroughly studied.

2. It was shown that the viscosity of the solution of the thickening compositions mainly depends on the concentration of the components and the time for modification, where an increase in viscosity is observed in the case of using modified starch. It was noted that the developed polymer thickening ingredients based on starch, carboxymethyl cellulose and sericin have good thixotropy and are stable for long-term storage.

References

1. Kozlova O. V., Pryajnikova V. G., Odinsova O. I. and others. Механохимические технололгии получения модифицированных крахмальных загусток.Journal Директор Россия Легпромбизнес. 2001.– № 4.– P. 60–64.
2. Ikhtiyarova G. A., Yariev O. M., Mavlonov B. A., Khaydarov A. A. О процессах омыления акриловой эмульсии с целью получения загустителя для печатания ткани Узб. хим.журн. 2002.– № 3.– P. 77–81.
3. Amonov M. R., Ikhtiyarova G. A., Yariev O. M., Ravshanov K. A. Загустки на основе природных и синтетических полимерных композиций для печатания тканей Узб.хим. журн. 2002.– № 4.– P. 71–77.
4. Ibragimova F. B., Amonov M. R., Ikhtiyarova G. A. Оценка влияния сродства композиции загустки на предел текучести и фиксации печатной краски.// Пластические массы.– М., 2002.– № 10.– 42 p.
5. Yariev O. M., Ibragimova F. B., Amonov M. R., Sodikova S. Sh. Полимерная композиция на основе реакции поликонденсации полифосфата калия с производными *α, γ* – дигалоидгидринглицерина / Журн. Уз. хим. – № 5. 2000. – P. 37–39.
6. Nazarov S. I., Amonova Kh. I., Amonov M. R., Ravshanova K. A. Печатно-технические свойства композиций на основе крахмала модифицированного с фосфатными соединениями // Журнал Композиционные материалы. – Tashkent, 2008. – № 2. – P. 36–39.
7. Nazarov S. I., Yariev O. M., Amonov M. R., Nazarov N. M. Применение фосфатного крахмала в качестве загустителя печатных красок // Journal Проблемы текстиля. – Tashkent, 2008. – 2. – P. 67–71.
8. Nazarov S. I., Yariev O. M., Nazarov I. I., Ravshanov K. A. Модифицирование крахмала для применения его при печатании тканей активными красителями // Uzbekchemicaljournal. – Tashkent, 2009. – №2. – P. 57–60.

https://doi.org/10.29013/AJT-19-11.12-48-51

Yakhshieva Zuhra Ziyatovna,
doctor of philosophy in chemistry,
Professor of Jizzakh State Pedagogical Institute
E-mail: yaxshiyeva67@mail.ru

Bakahonov Anvar Akobirobvich,
Lecturer of Department of Chemistry Teaching Methodology,
Jizzakh State Pedagogical Institute

Kurbonova Dilafruz Sobirovna,
holder of master's degree, Jizzakh State Pedagogical Institute

OPTIMIZATION OF AMPEROMETRIC CONDITIONS FOR THE DETERMINATION OF MOLYBDENUM IONS IN ANTHROPOGENIC OBJECTS

Abstract. The current-voltage behavior in the selected medium on the corresponding electrode of both titratable molybdenum ions and an organic reagent, as well as all other components of the analyzed solution involved in the titration during optimization of amperometric titration conditions, is investigated. We studied the electrochemical behavior of N-methylanabazine – α-azo-β-naphthol, on a platinum disk microanode; oxidation curves taken at different temperatures of the test solution and the number of revolutions of the platinum disk microanode in all studied buffer mixtures and background electrolytes; the diffusion nature of the limiting current of the electrooxidation of the reagents and the cathodic reduction of titrated metal ions is established, and their irreversible nature is established by the method of logarithmic analysis. On their basis, methods have been developed for the amperometric titration of molybdenum ions with one or two indicator electrodes in aqueous, non-aqueous, mixed media.

Keywords: amperometry, amperometric titration, organic reagents, expressivity, titration, selectivity, selectivity, correctness, reproducibility, electrical conductivity.

Relevance. The growing demand for molybdenum and its alloys is linked with the development of such industries as instrument manufacturing, electronics, nuclear and electric power industry – determinants of the technological progress of the whole world, which makes the problem of analysis of environmental objects with micro-content of this metal relevant. Accuracy, correctness and reproducibility, along with the rapidity of determination, are especially important because of the high demand of the determined molybdenum for both its biological and physiological properties.

The importance of molybdenum in science, technology, industry and the national economy is enormous, as it possesses unique properties and original characteristics. This in turn requires the improvement of existing methods for determining molybdenum, the development of new methods with the aim of establishing their macro-, micro- and trace concentrations in anthropogenic objects, since their micro-quantities play an important and decisive role in solving various analytical, electrochemical, medical, environmental and other tasks.

Based on the third direction of the Strategy for the Further Development of the Republic of Uzbekistan, aimed at "rising industry to a new level, further intensifying the production of finished products based on deep processing of local raw materials, mastering the production of fundamentally new types of products and technologies", the main tasks are determined. The regulatory measures taken in this direction have achieved certain results, especially, high-level scientific research has been organized and large-scale measures have been taken to ensure the import and substitution of chemical reagents for the local market. The amperometric method of analysis is based on establishing the end point of titration by the diffusion anode or cathode current, while measuring the current passing through the cell at a certain potential difference (ΔE) on the electrode. This current is considered as a function of a useful analytical signal from the volume (concentration) of the titration solution – N-methylanabazine – α-azo-β-naphthol. An indicator electrode for amperometric titration of metals is a rotating solid platinum electrode. Such titration is based on the same laws as in quantitative polarography and voltammetry, where a direct proportional (linear) relationship between the diffusion current and the concentration of the analyzed substance is observed.

After conducting preliminary experiments for optimization of molybdenum ions titration conditions, the influence of the external voltage, the nature and concentration of the background electrolyte and the buffer mixture, as well as foreign cations interfering with anions and complex compounds, were studied.

The experiment were conducted under the following conditions: electrode voltage: 0.75 V, test solution volume – 10 ml, temperature – RT(20–25 °C), titrant concentration 0.01 M.

To increase the electrical conductivity of the titratable medium and improve the shape of the curves for the determination of molybdenum (VI) with a solution of N-methylanabazine – *α*-azo-*β*-naphthol, we studied the effect of various concentrations of buffer mixtures and background electrolytes, which significantly increase the accuracy of the data and the reproducibility of the developed methods. The effect of various background electrolytes and buffer mixtures in the range of pH 1.60–12.50 was investigated.

The electrochemical determination of molybdenum (VI) with a solution of N-methylanabazine – α-azo-β-naphthol was studied on the background of hydrochloric, nitric, perchloric, sulfuric acids, in a Britton-Robinson buffer and solutions of alkali metal chlorides. It was shown that molybdenum (VI) is well titrated in all studied background electrolytes, forming strong complex compounds with N-methylanabazine – α-azo-β-naphthol, therefore, its electrochemical behavior was studied on the background of hydrogen chloride, perchloric and sulfuric acids, sodium chlorides and potassium, a Britton-Robinson buffer in a pH range of 1.62–12.5. The maximum sensitivity, correctness and reproducibility of the determination of molybdenum (VI) with a solution of N-methylanabazine – *α*-azo-*β*-naphthol are observed in strongly acidic media, and experiments have shown that amperometric determination of molybdenum (VI) is possible even in the presence of concomitant cations, and the best background the electrolyte is 1.0 M potassium chloride, because only on it the best results were obtained.

To improve the shape of the curves and increase the electrical conductivity of the titrated medium, as well as to suppress migration currents when determining molybdenum (VI) with a solution of N-methylanabazine – *α*-azo-*β*-naphthol, the effect of the universal Britton-Robinson buffer in the pH range of 1.81–12 was also studied.

A series of experiments aimed at clarifying the nature of the influence of this factor on the conditions of amperometric titration of molybdenum (VI) with a solution of N-methylanabazine – *α*-azo-*β*-naphthol was carried out at their concentrations equal to 0.2 M in the volume of titrated solution equal to 10.0 ml, at the temperature of the test solution 20 ± 6 °C.

The calculation of the found amount of metal (component) in the titrated sample was carried out according to the formula known used in literature:

$$P = V_{TAA} \times m \times N \times 1000 \text{ mg};$$

where: V_{TAA} – is the volume of reagent used for titration (ml);

m – is the coefficient of the piston microburette (0.0029 ml);

N – is the equivalent mass of the titrated metal.

It was experimentally established that the best results when titrating molybdenum with a solution of N-methylanabazine are observed in acidic media at pH 1.81–2.82, resulting in the formation of strong complex compounds.

Since the voltage value should have a significant effect on the type of curves, conditions and results of metal determination, we studied the effect of the voltage value on titration of molybdenum (VI) with a solution of N-methylanabazine – *α*-azo-*β*-naphthol under the following optimal conditions: background – universal buffer with a pH of 1.81–2.62, the concentration of titrant is 0.001 M, the volume of the titrated solution is 8–10.0 ml, the temperature is about 24 °C. The voltage on the platinum indicator electrodes was changed in the range of 0.20–1.25 V in steps of 0.25 V.

The results of the experiment show that the average value of the titrant consumption at the titration endpoint depends on the voltage supplied to the indicator electrodes, where the average titrant consumption at the titration endpoint depends on the potential difference (ΔE) supplied to the platinum indicator electrodes.

Determination of molybdenum (VI) with a solution of N-methylanabazine – *α*-azo-*β*-naphthol in various real industrial materials and natural objects is a necessary and urgent task of modern electroanalytical chemistry. Therefore, the possibility and optimized conditions of amperometric titration of molybdenum (VI) with a solution of N-methylanabazine – *α*-azo-*β*-naphthol in a wide range of their concentrations have been shown and optimized, and with appropriate selection of the determination conditions, it becomes sensitive and highly selective.

For a successful study, the influence of the potential supplied to the indicator electrodes (0.25–1.25 V) on the shape of the curves, conditions and results of amperometric titration of molybdenum (VI) with a solution of N-methylanabazine – *α*-azo-*β*-naphthol was studied. As a rule, the concentration of the titrating reagent should be several orders of magnitude higher than the content of the metals being determined. The titrant is added in small portions of a precision piston microburette, due to which dilution of the test solution can be neglected.

It was found that the curves that are optimal in shape and the best titration results are observed at a potential difference (ΔE) on a platinum indicator electrode equal to 0.75 V.

The experimental results obtained indicate that the developed amperometric methods for the determination of molybdenum (VI) ions with a solution of N-methylanabazine – *α*-azo-*β*-naphthol are distinguished by high metrological characteristics and analytical parameters that allow them to be recommended in the analysis of real materials, ores, alloys, minerals, tails and other objects.

Summing up the results of the studies, it is necessary to note that the obtained experimental data served as the basis for the development of amperometric methods for the determination of ions of the studied noble metals in their model binary, ternary and more complex mixtures that simulate natural objects and industrial materials, thereby showing the possibility of their real practical application in the analysis of objects environment and industrial materials.

References:

1. Гохштейн Я. П. Использование вращающегося твердого электрода // – М.; Наука. 1987.– 239 с.
2. Лурье Ю. Ю. Справочник по аналитической химии // – М.: Химия. 1979.– С. 230–236.

3. Геворгян А. М., Яхшиева З. З. Оптимизация условий амперометрического определения некоторых благородных металлов раствором тиоацетамида. // Хим. Пром.– Санк-Петербург. 2010.– Т. 87.– № 2.– С. 85–88.
4. Бимиш Ф. Аналитическая химия благородных металлов // В 2-х частях. 2-я кн.,– М.; Мир. 1989.– 399 с.
5. Хайдукова М. М. Новые подходы к постановке эксперимента и обработке данных в потенциометрическом мультисенсорном анализе // Дисс. на соиск. уч. ст. к.х. н.– Санкт-Петербург. 2016.– С. 130–135.
6. Терещенко П. Н. Применение графитовых электродов при анализе объектов окружающей среды // – М.; Наука.– 1991.– С. 212–220, 300.
7. Yakhshieva Z. Amperometric determination of some metals sulfur-containing organic reagents in non-aqueous, and mixed aqueous media // Austrian Journal of Technical and Natural Science.– Austria. 2015.– № 5–6.– P. 151–154.

Section 6. Electrical engineering

https://doi.org/10.29013/AJT-19-11.12-52-61

Baghdasaryan Marinka,
Professor, Doctor of Department of Electrical Machines and Apparatuses, National Polytechnic University Of Armeni
E-mail: m.baghdasaryan@seua.am

Sargsyan Sargis,
Post-graduate student,
National Polytechnic University of Armeni
E-mail: 229532@inbox.ru

Hakobyan Tigran,
Post-graduate student,
National Polytechnic University of Armeni
E-mail: tighak@gmail.com

A RESEARCH MODEL FOR THE OPERATING MODES OF THE MECHANICAL PART OF THE ORE CRUSHER ELECTRICAL DRIVE SYSTEM

Abstract. A simulation model, allowing to study and evaluate the operating modes of mechanical transfer link of an induction electrical drive system that ensures the operation of ore crusheris developed. The model was implemented in the Simulink environment of the MatLab software package and can be successfully used to identify the defects in the mechanical part of the induction electrical drive systems operating with the percussive application of a load, and to make decisions aimed at improving the operating conditions.

Keywords: simulation model, percussive load, mechanical part, elastic link, operating mode, rigidity.

Introduction. The electrical drive systemresearch model should reflect the peculiarity of the structural scheme of the given system, as well as the loading mode. Taking into account the structural diversity of electrical systems and the variety of technological load changing, it is of scientific and technical interest to develop a model for the study of the working modes of the mechanical part of the electrical drive system with percussive load.

There are numerous works which are devoted to the modeling and investigation of different links of the electrical drive system [1–4].

Ivanchenko's monographs devoted to the investigation of the dynamic phenomena occurring during the operation of metallurgical machines are of particular interest [1; 2]. In these works, the development of the mathematical models for investigation

the transient processes and the steady state of single-motor and multi-motor electrical drive systems has been considered.

Rational parameters providing transient attenuation and reduction of electric drive system dynamics are obtained. Mathematical models have been developed for technological mechanisms with a constant and variable load changing with certain regularity.

In the work devoted to the study of the mechanical subsystem of the electrical drive system with a reducer [3], transient functions for the main regulated coordinates were obtained.

The torque of resistance created by some technological mechanisms operating with the percussive load has a random character and a specific form whose impact on the mechanical part of the electrical drive system needs a comprehensive study. Such a special torque of resistance is created by the ore crushers widely used in mining and metallurgical industry. That is why, in the present paper, a model for researchthe mechanical part of the electrical drive system has been developed.

The **goal of the work** is to develop the research model of the mechanical part of the ore crusher electrical drive system which will give an opportunity to estimate the change in the operation modes of the mechanical transfer links of the system and reveal the possible defects.

The obtained results. In practice, an asynchronous electrical drive is used for ore crushers. The mathematical description of the mechanical part of the asynchronous electrical drive system of the ore crusher can be represented in the form of a system of differential equations given below:

$$\begin{cases} J_1 \dfrac{d\omega_1}{dt} - M_{12} = -M_c \\ J_2 \dfrac{d\omega_2}{dt} + M_{12} = M_D - \beta\omega_2 \\ M_{12} = \dfrac{c_1}{p}\left(\omega_2 - \omega_1\right), \end{cases} \quad (1)$$

where J_1 and J_2 are the moments of inertia of the crusher and the induction motor rotor's respectively; c_1 is the rigidity of the drive link between the crusher and the electric motor; ω_1 and, ω_2 are the angular speeds rotation of the crusher and the motor respectively; M_c is the torque of resistance of the crusher load; M_D is the torque of the induction motor; M_{12} is the load torque of the elastic element; β is the rigidity of the motor characteristics.

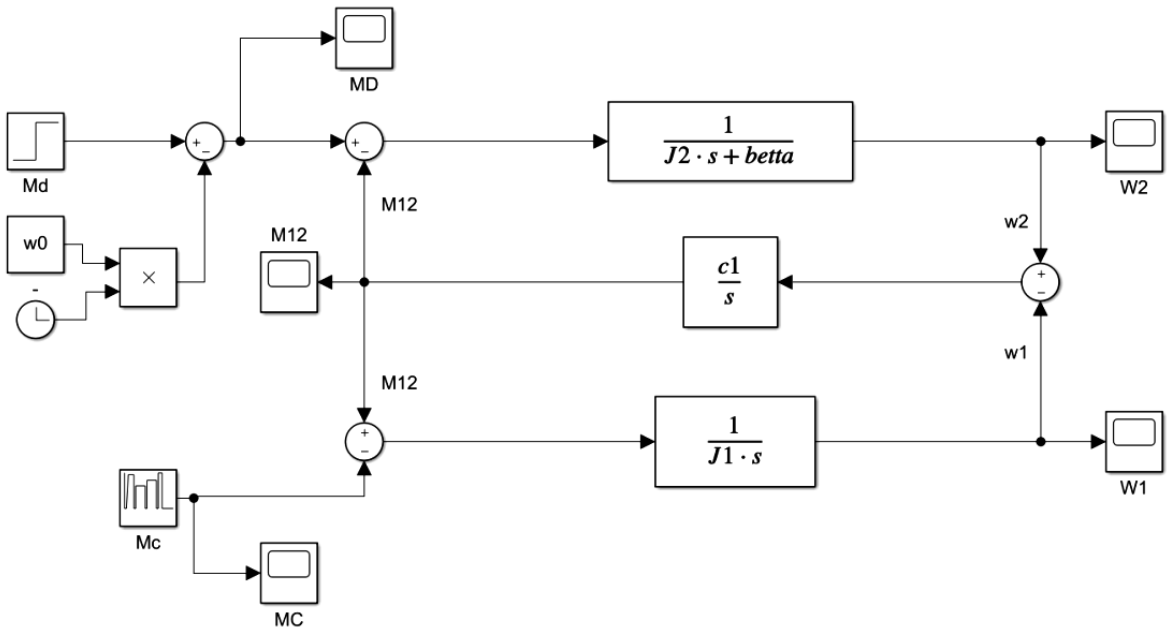

Figure 1. The structural scheme of the crusher's electrical drive elastic subsystem

Using the system of differential equations (1), the structural scheme of the elastic subsystem has been obtained (Fig. 1). The scheme has been plotted in the Simulink environment of the MatLab software package [5; 6].

In the structural scheme given in Fig. 1, the form of change in load resistance torque M_c was chosen taking into account the operating mode of crushers used in the mining and metallurgical industry.

The torque of resistance created by the crusher over timeundergoes a random change. The conical crushers which have found wide application operate in a continuous mode, while the jaw crushers – in a discontinuous mode. Taking into account the abovementioned, to develop a model for investigating the operation modes of the system's mechanical part, the form of the torque M_c change presented in (Fig. 2) has been used.

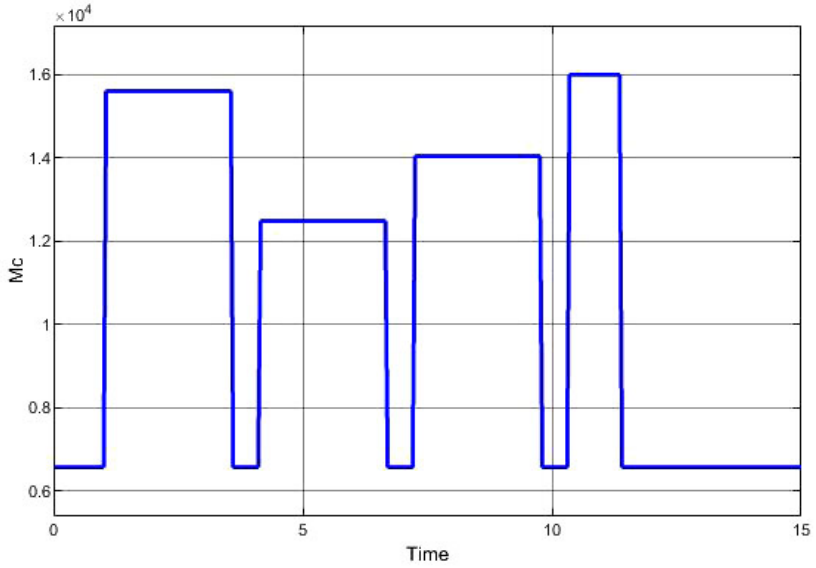

Figure 2. The form of the change of the crusher's M_c torque of resistance

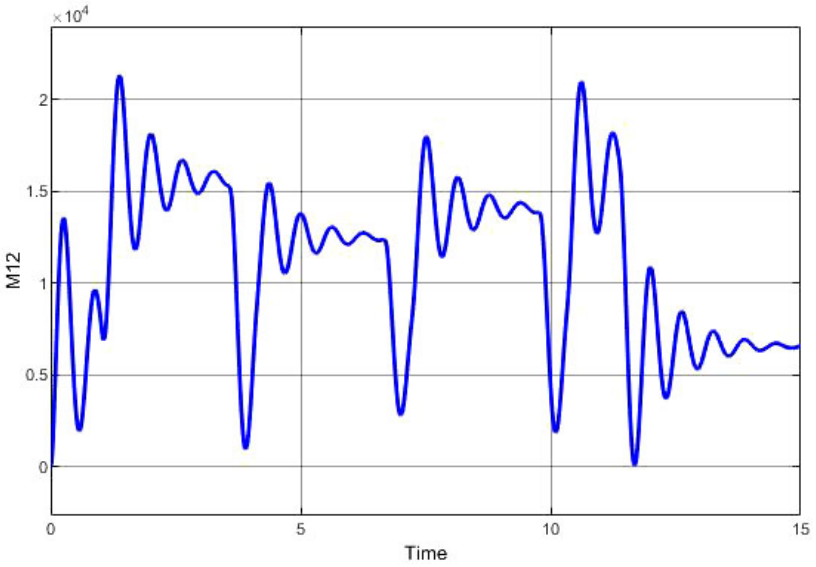

Figure 3. The change of the elastic element load torque at $c_1 = 25500 kg.m/rad$

It is known that the insufficient rigidity of the shaft causes bending in the gear transmission which leads to a non-uniform distribution of the load on the gear teeth.

The insufficient rigidity of the parts increases friction and pressure in the movabile conjugation.

Taking into account that the above phenomena can contribute to the emergence of emergency modes, in this work the characteristics of the mechanical part of the system have been considered for different rigidities of the transmission link.

By means of the model presented in (Fig. 2), the M_{12} torque changes in time at different values of the c_1 rigidity of the transmission link have been obtained (Fig. 3, 4).

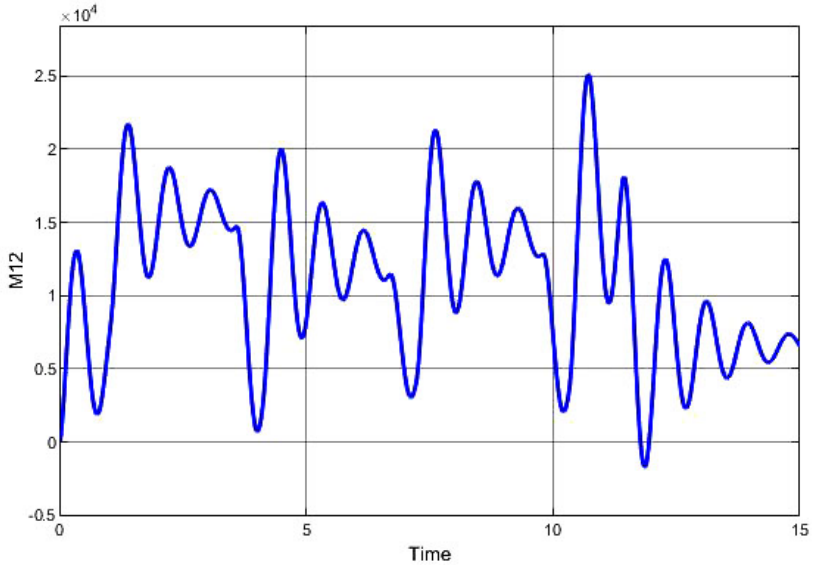

Figure 4. The change of the elastic element load torque at $c_1 = 15000 kg.m/rad$

From Figures 3 and 4, it can be seen that the decrease in the rigidity of the c_1 link brings about the intensity of the M_{12} torque change.

The transfer function $W(s) = M_{12}(s)/M_D(s)$ of the electrical drive elastic subsystem has been derived for different values of c_1 rigidity of the transmission link.

$$W(s) = \frac{68s}{s^3 + 24,4s^2 + 159,1s + 2222},$$

when

$$c_1 = 25500 kg.m/rad, \quad (2)$$

The characteristic equation has the following form:

$$s^3 + 24,4s^2 + 159,1s + 2222 = 0$$

whose solutions are:

$$s_1 = -21,7808; \quad s_2 = -1,3096 + j10,0154;$$
$$s_3 = -1,3096 - j10,0154$$

For the characteristic equation, the obtained roots are left to the false axis, which shows that the system is stable:

$$W(s) = \frac{40s}{s^3 + 24,4s^2 + 93,57s + 1307}, \text{ when}$$
$$c_1 = 15000 кг.м/рад, \quad (3)$$

The characteristic equation of the transfer function (3) has the following form:

$$s^3 + 24,4s^2 + 93,57s + 1307 = 0,$$

whose solutions are:

$$s_1 = -22,8101; \; s_2 = -0,7950 + j7,5282;$$
$$s_2 = -0,7950 - j7,5282.$$

The obtained results show that the system is stable.

To investigate the system, the amplitude-frequency and phase-frequency characteristics of the function are obtained (Fig. 5). For that, $s = j\omega$ is placed in the $W(s)$ transfer function. The obtained function $W(j\omega)$ consists of real and false components. The $W(j\omega)$ frequency transfer function can be presented in the following form:

$$W(j\omega) = A(\omega)e^{j\phi(\omega)},$$

where $A(\omega)$ is the amplitude-frequency characteristic of the system which shows how much the output signal amplitude is higher than the input signal amplitude; $\phi(\omega)$ is the phase-frequency characteristic which shows the magnitude of the phase shift of the output and input signals for a fixed frequency.

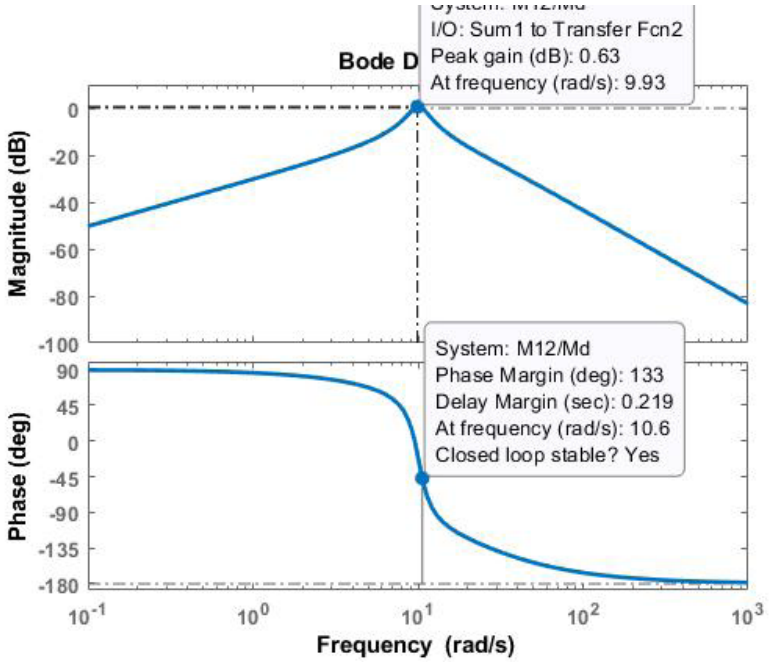

a)

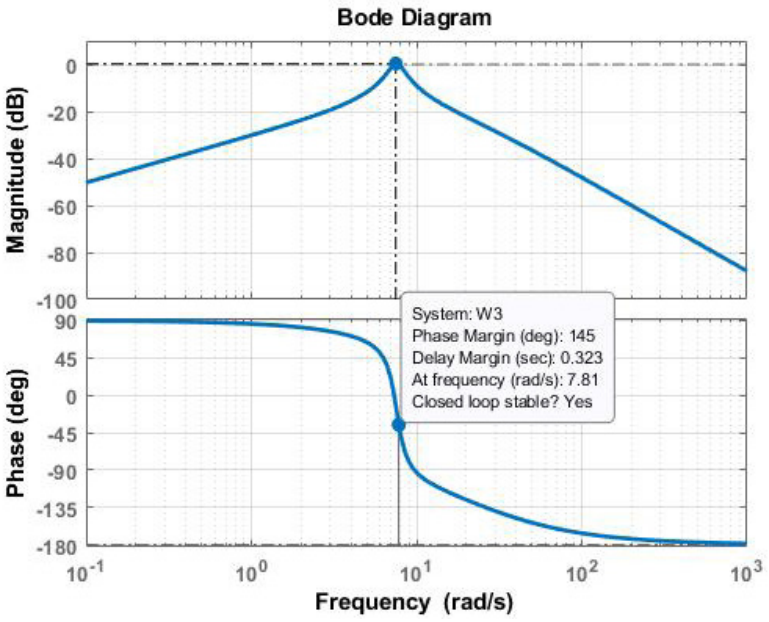

b)

Figure 5. The logarithmic form of the amplitude-frequency and phase-frequency characteristics of the transfer function: a) $c_1 = 25500 kg.m/rad$; b) $c_1 = 1500 kg.m/rad$

Taking into account the fact that the Nyquist criterion gives an opportunity to follow the impact of the change in the transfer function parameters on the system stability, the Nyquist curves of the W transfer func-

tion for different values of the link rigidity have been obtained (Fig. 6). From the curves, one can see that in case of the frequency change in the range from 0 to $+\infty$, the phase-amplitude characteristics of the open-loop system do not include the $(-1, j0)$ coordinate (Fig. 6), from what it follows that the given system is stable.

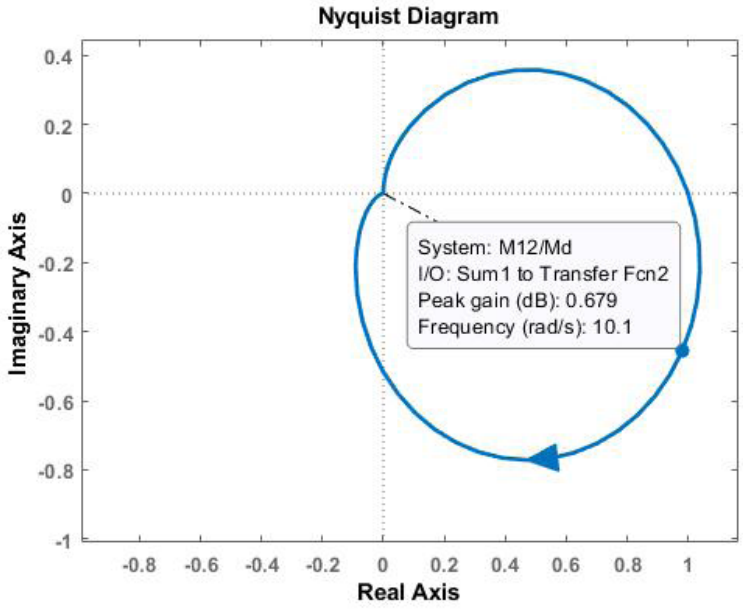

a)

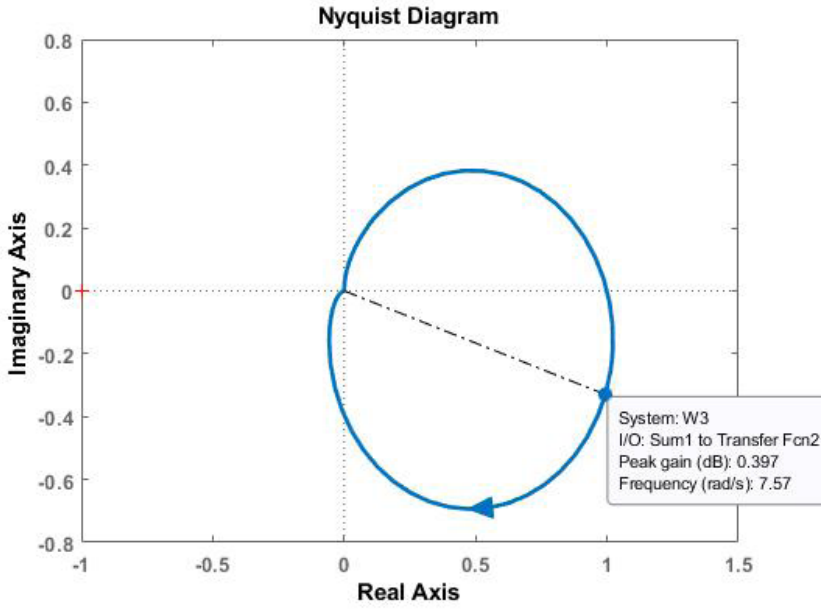

b)

Figure 6. The Nyquist curves of the W transfer function for different values of the link rigidity: a) $c_1 = 25500 kg.m/rad$; b) $c_1 = 15000 kg.m/rad$

From (Fig. 7), it can be seen that in case of the c_1 decrease, the period of stabilization increases.

The transfer function $G(s) = M_{12}(s)/M_c(s)$ of the electrical drive`s elastic subsystem for different

values of the c_1 rigidity of the transmission link have been derived:

$$G_1(s) = \frac{91,07s + 2222}{s^3 + 24,4s^2 + 159,1s + 2222}, \quad (4)$$

when $c_1 = 25500 kg.m/rad$,

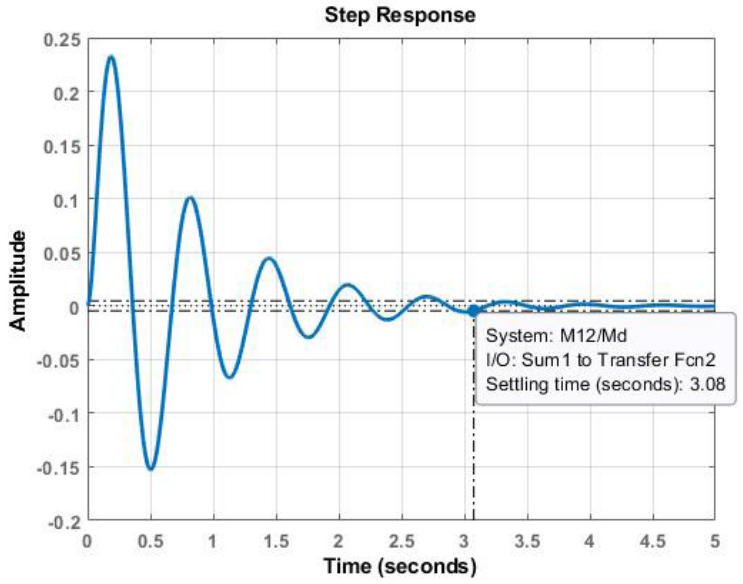

a)

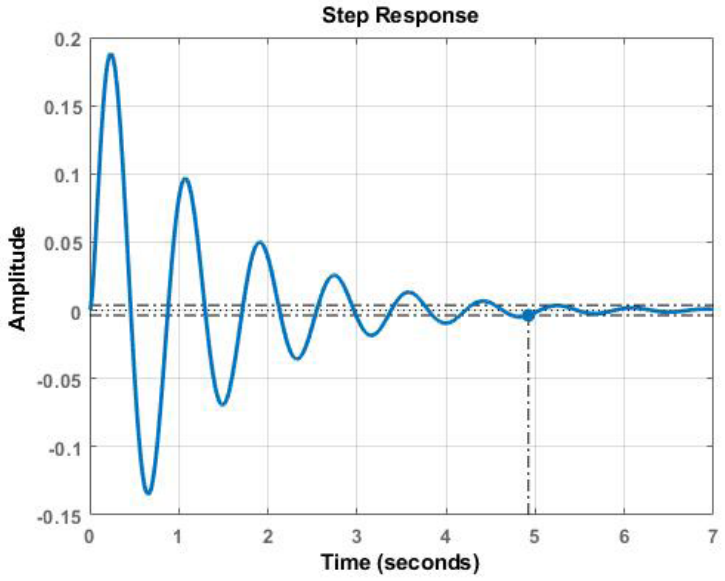

b)

Figure 7. The curves of the transient process of the F transfer function: a) $c_1 = 25500 kg.m/rad$; b) $c_1 = 15000 kg.m/rad$

The roots of the characteristic equation $s^3 + 24,4s^2 + 159,1s + 2222 = 0$, are $s_1 = -21,7808$; $s_2 = -1,3096 + j10,0154$; $s_2 = -1,3096 - j10,0154$.

$$G_1(s) = \frac{53,57s + 1307}{s^3 + 24,4s^2 + 93,57s + 1307},$$
$$c_1 = 15000\,kg.m/rad, \quad (5)$$

The roots of the characteristic equation

$$s^3 + 24,4s^2 + 93,57s + 1307 = 0$$

are $s_1 = -22,8101$; $s_2 = -0,7950 + j7,5282$; $s_2 = -0,7950 - j7,5282$.

From the roots obtained for the characteristic equations it follows that for both values of the link rigidity c_1 the system is stable.

For studying the system the amplitude-frequency and phase-frequency characteristics of the function $G_1(s)$ have been obtained (Fig. 8). For that, $s = j\omega$ is placed in the $G_1(s)$ transfer function.

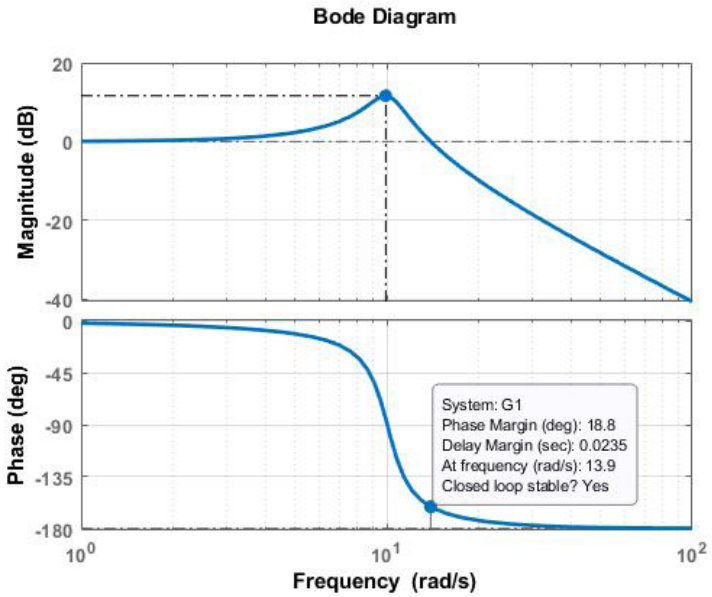

a)

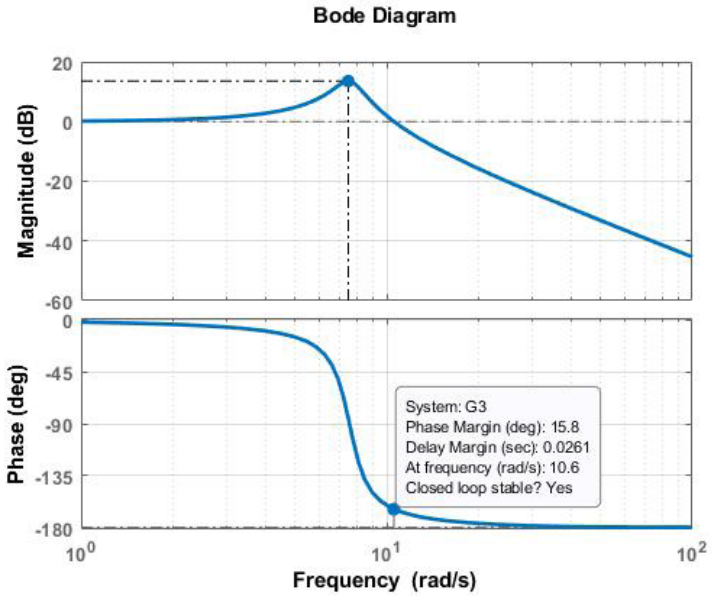

b)

Figure 8. The logarithmic form of the amplitude-frequency and phase-frequency characteristics of the G transfer function: a) $c_1 = 25500\,kg.m/rad$; b) $c_1 = 15000\,kg.m/rad$

In (Fig. 9), the form of the G transfer function transient process for different values of the c_1 link rigidity is represented, from what it follows that along with the c_1 decrease, the time of the system stabilization increases.

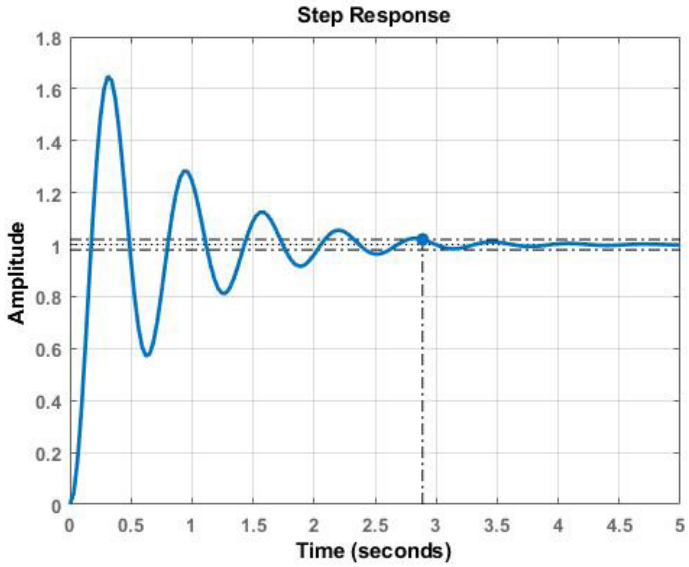

a)

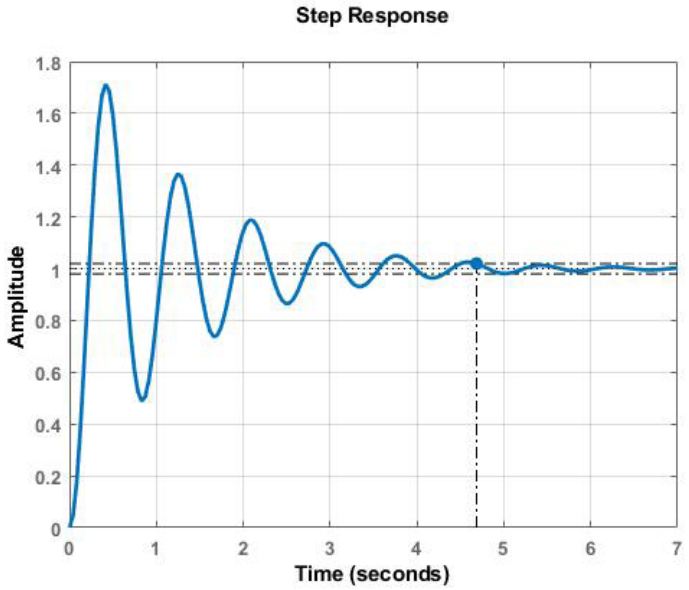

b)

Figure 9. The form of the G transfer function transient process: a) $c_1 = 25500 kg.m/rad$; b) $c_1 = 15000 kg.m/rad$

Conclusion

The developed simulation model allows to carry out a comprehensive study and evaluation of the working condition of the mechanical part of the asynchronous electric drive system, and make decisions that will prevent the system from appearing in irregular operating modes.

References:

1. Ivanchenko F. K., Krasnoshapka V. A. Dynamics of metallurgical machines.– M.: Metallurgy, 1983.– 294 p.
2. Ivanchenko F. K., Krasnoshapka V. A. Applied problems of machine dynamics. – Kiev: Visha shkola, 1983.– 200 p.
3. Koval A. S. Lagun N. S. Transfer functions of the mechanical subsystem of the reducer electric drive of elevators // Bulletin of the Belarusian-Russian University.2015.– No. 2 – P. 112–118.
4. Kim E., Tan A. S. S., Kosse V., Howard I., and Tan T. Monitoring of low-speed machines. CIEAM Final. Project report, ID202, 2010.
5. Chernikh I. V. Modelling of electrical devices in MATLAB, SimPower Systems and Simulink.–St.-Pt.: Piter, 2008.– 290 p.
6. Terekhin V. B. Modelling of electric drive systems in Simulink (Matlab7.0.1): – Tomsk: Publ. House of the Tomsk Polytechnic University, 2008.– 320 p.

Contents